

## PRESOLAR SiC GRAINS OF TYPE A AND B: THEIR ISOTOPIC COMPOSITIONS AND STELLAR ORIGINS

SACHIKO AMARI, LARRY R. NITTLER,<sup>1</sup> AND ERNST ZINNER

Laboratory for Space Sciences and the Physics Department, Washington University, St. Louis, MO 63130-4899; sa@howdy.wustl.edu, ekz@howdy.wustl.edu

KATHARINA LODDERS

Department of Earth and Planetary Sciences, Washington University, One Brookings Drive, St. Louis, MO 63130-4899; lodders@levee.wustl.edu

AND

ROY S. LEWIS

Department of Earth and Planetary Sciences, Chicago, IL 60637-1433; r-lewis@uchicago.edu

Received 2001 April 5; accepted 2001 May 24

### ABSTRACT

A total of 124 presolar SiC grains of type A and B (defined as having  $^{12}\text{C}/^{13}\text{C} < 10$ ) were identified by ion imaging in an acid-resistant residue of the Murchison carbonaceous meteorite. Their isotopic ratios, together with those of 28 previously analyzed A + B grains, are reported here. The  $^{14}\text{N}/^{15}\text{N}$  ratios range from 39 to  $10^4$ , with one-third of the grains having  $^{14}\text{N}/^{15}\text{N}$  ratios lower than the solar value of 272. Inferred  $^{26}\text{Al}/^{27}\text{Al}$  ratios of A + B grains range up to  $10^{-2}$ . These isotopic compositions clearly distinguish A + B grains from other presolar SiC populations. Among the A + B grains, grains with lower  $^{12}\text{C}/^{13}\text{C}$  ratios tend to have lower  $^{14}\text{N}/^{15}\text{N}$  and higher  $^{26}\text{Al}/^{27}\text{Al}$  ratios. Silicon of A + B grains is enriched in the neutron-rich isotopes ( $^{29}\text{Si}/^{28}\text{Si}$  up to 1.20 times solar,  $^{30}\text{Si}/^{28}\text{Si}$  up to 1.13 times solar), and in an Si three-isotope plot the distribution of the isotopic ratios is very similar to that of mainstream grains, indicating that the parent stars of the A + B grains had close-to-solar metallicity. Titanium isotopic ratios of 13 grains, out of 30 analyzed, deviate from solar by more than  $2\sigma$  in at least one isotopic ratio and span the same range as those of mainstream grains. Trace element abundance patterns of 20 previously measured A + B grains indicate that seven condensed from an atmosphere without *s*-process enrichments, while 13 did so from an atmosphere enriched in *s*-process elements by 3–5 times solar. Observationally, the most likely sources of A + B grains with solar *s*-process abundances are J-type carbon stars, but the origin of these stars is unclear. Born-again asymptotic giant branch (AGB) stars, typified by Sakurai's object (V4334 Sgr), are possible sources of A + B grains with enhanced *s*-process elemental abundances. Other C-rich stars with low  $^{12}\text{C}/^{13}\text{C}$  ratios including R stars and CH stars are less likely stellar sources. Whatever the stellar sources, both H and He burning as well as mixing must have occurred in the proper combination to produce both low  $^{12}\text{C}/^{13}\text{C}$  ratios and  $\text{C} > \text{O}$  in the envelope. A special nucleosynthetic problem is posed by the  $^{14}\text{N}/^{15}\text{N}$  ratios of the grains. High ratios can be explained by hot bottom burning and by cool bottom processing in thermally pulsing AGB stars. Another proposed scenario that possibly yields this signature is extensive mixing of He-burning material into the H-rich envelope during the core He flash. However, the spread of the  $^{14}\text{N}/^{15}\text{N}$  ratios and lower-than-solar  $^{14}\text{N}/^{15}\text{N}$  ratios remains unexplained. The isotopic and elemental compositions of A + B grains can provide new information about nucleosynthesis in their possible parent stars that cannot be obtained in any other way.

*Subject headings:* dust, extinction — ISM: abundances —  
nuclear reactions, nucleosynthesis, abundances — stars: AGB and post-AGB

*On-line material:* machine-readable table

### 1. INTRODUCTION

Diamond was the first type of presolar dust isolated from meteorites (Lewis et al. 1987). This discovery was followed by those of presolar silicon carbide (SiC) (Bernatowicz et al. 1987; Tang & Anders 1988), graphite (Amari et al. 1990), refractory carbides such as TiC (Bernatowicz et al. 1991, 1996), oxides (corundum =  $\text{Al}_2\text{O}_3$ , spinel =  $\text{MgAl}_2\text{O}_4$ , and hibonite =  $\text{CaAl}_{12}\text{O}_{19}$ ) (Huss et al. 1994; Hutcheon et al. 1994; Nittler et al. 1994, 1997; Choi et al. 1998; Choi, Wasserburg, & Huss 1999), and silicon nitride ( $\text{Si}_3\text{N}_4$ ) (Nittler et

al. 1995). Presolar grains are surviving star dust in primitive meteorites, which have experienced little metamorphism since they formed 4.5 billion years ago during the earliest stages of the solar system. These grains remained intact throughout the journey from their parent stars and survived the formation of the solar system. Review papers on presolar grains and their implications for astrophysics can be found in Bernatowicz & Zinner (1997; see also Anders & Zinner 1993; Zinner 1998).

Isotopic analysis of individual presolar grains by secondary ion mass spectrometry (SIMS) has shown that their isotopic ratios are, in general, vastly different from the ratios observed in material of known solar system origin and sometimes span more than 3 orders of magnitude (Zinner 1998). Such huge isotopic anomalies can be pro-

<sup>1</sup> Department of Terrestrial Magnetism, Carnegie Institution of Washington, 5241 Broad Branch Road NW, Washington, DC 20015; lrn@dtm.ciw.edu.

duced only by nucleosynthesis in stars and are proof of the stellar origin of the grains. The isotopic compositions of the grains thus provide information about specific stages in the evolution of their parent stars.

After diamond, SiC is the most abundant type of presolar dust in meteorites. Still, its concentration in primitive meteorites is only 6 parts per million (ppm) (Amari, Lewis, & Anders 1994). Silicon carbide has been classified into several different populations on the basis of the C, N, and Si isotopic ratios measured in single grains with the ion microprobe (Figs. 1 and 2) (Hoppe et al. 1994; Hoppe & Ott 1997). Most grains (~93%) are defined as “mainstream” grains and have isotopically heavy C ( $^{12}\text{C}/^{13}\text{C} = 20\text{--}100$ ), light N ( $^{14}\text{N}/^{15}\text{N} > 272 = \text{solar}$ ), and Si enriched in the neutron-rich isotopes. Analyses of SiC bulk samples ( $\equiv$  aggregates of many grains) have shown pronounced *s*-process signatures for the noble gases Kr and Xe (Lewis, Amari, & Anders 1990, 1994; Gallino et al. 1990) and for Sr (Podosek et al. 2001), Ba (Ott & Begemann 1990; Zinner, Amari, & Lewis 1991; Prombo et al. 1993; Gallino, Raiteri, & Busso 1993), Nd (Zinner et al. 1991; Richter, Ott, & Begemann 1993), and Sm (Zinner et al. 1991; Richter et al. 1993). Bulk analyses include minor populations of SiC grains. However, with few exceptions, the bulk isotopic signatures are dominated by the population of mainstream grains. Recently, measurements of heavy-element isotopic ratios in individual grains by resonance ionization mass spectrometry (RIMS) have revealed *s*-process Zr (Nicolussi et al. 1997) and Mo (Nicolussi et al. 1998) in mainstream

SiC grains. Thermally pulsing asymptotic giant branch (TP-AGB) stars are believed to be the source of the main *s*-process component in the solar system elemental abundance distribution, indicating that such stars are the most likely stellar sources of the mainstream grains (e.g., Gallino, Busso, & Lugaro 1997). The isotopic ratios of the light elements C and N also point to an AGB star origin (Gallino et al. 1994; Hoppe et al. 1994; Lugaro et al. 1999).

Grains of type Y (~1% of total SiC) are defined as having  $^{12}\text{C}/^{13}\text{C}$  ratios larger than 100 and enrichments in  $^{30}\text{Si}$  compared with mainstream grains (Figs. 1 and 2) (Amari et al. 2001b), while Z grains (~1% of total SiC) show a similar range of  $^{12}\text{C}/^{13}\text{C}$  ratios as mainstream grains do but have larger  $^{30}\text{Si}$  excesses than Y grains (Hoppe et al. 1997a, 1997b). Amari et al. (2001b) have proposed that Y grains formed in AGB stars of approximately half solar metallicity ( $Z = 0.01$  or  $[\text{Fe}/\text{H}] = -0.3$ ) with masses ranging from 1.5 to possibly  $5 M_{\odot}$ . Hoppe et al. (1997a, 1997b) have suggested that Z grains formed in low-mass ( $M < 2.3 M_{\odot}$ ), low-metallicity ( $Z = 0.006$  or  $[\text{Fe}/\text{H}] = -0.52$ ) AGB stars that had experienced extra mixing (Charbonnel 1995; Wasserburg, Boothroyd, & Sackmann 1995). From the Si isotopic compositions of those three populations of SiC grains, Zinner et al. (2001) have concluded that they formed in TP-AGB stars with a range of metallicity, from close-to-solar metallicity for mainstream grains down to metallicity  $Z \approx 0.006$  for Z grains.

Silicon carbide grains of type X (~1% of total SiC) are characterized by isotopically light C, heavy N, high  $^{26}\text{Al}/^{27}\text{Al}$  ratios (~0.1–0.6), and  $^{28}\text{Si}$  excesses up to 5 times solar (Amari et al. 1992; Nittler et al. 1995; Hoppe et al. 2000).  $^{44}\text{Ca}$  excesses, originating from the decay of  $^{44}\text{Ti}$  ( $T_{1/2} = 60$  yr), have been observed in several grains (Nittler et al. 1996; Hoppe et al. 1996a). Since  $^{44}\text{Ti}$  is produced by explosive nucleosynthesis in supernovae (SNe), its inferred former presence in the grains is proof of their SN origin. Low-density graphite grains have isotopic signatures similar to those of X grains, also implying an SN origin (Amari, Zinner, & Lewis 1995b, 1996b; Travaglio et al. 1999a). Travaglio et al. (1999a) have performed mixing calculations of different layers of the SN models by Woosley & Weaver (1995) in an attempt to reproduce the isotopic signatures of the low-density graphite grains. Although many general signatures can be reproduced, several problems remain and are discussed in detail by Travaglio et al. (1999a).

A few grains have low  $^{12}\text{C}/^{13}\text{C}$ ,  $^{14}\text{N}/^{15}\text{N}$ , high inferred initial  $^{26}\text{Al}/^{27}\text{Al}$ , and  $^{30}\text{Si}$  excesses, relative to solar system ratios, indicative of an origin in nova ejecta (Amari et al. 2001a).

Grains of type A and B comprise ~3%–4% of presolar SiC and are defined as having  $^{12}\text{C}/^{13}\text{C}$  ratios of less than 10. Type A grains have  $^{12}\text{C}/^{13}\text{C}$  ratios of less than 3.5 (the equilibrium value of the CNO cycle), and B grains have ratios between 3.5 and 10 (Hoppe et al. 1994, 1996b; Amari et al. 1997, 1999, 2000). However, since this is an ad hoc division and since the other isotopic features are very similar in both populations of grains, they will be treated as a single population (“A + B”) in this paper. Although A + B grains are not as rare as X, Y, and nova grains, they still comprise only a minor proportion of presolar SiC in meteorites. The study of a statistically significant number requires that the grains be found in an efficient way. Here we report C, N, Al, Si, and Ti isotopic ratio measurements of 121 A + B grains, identified by automatic high mass

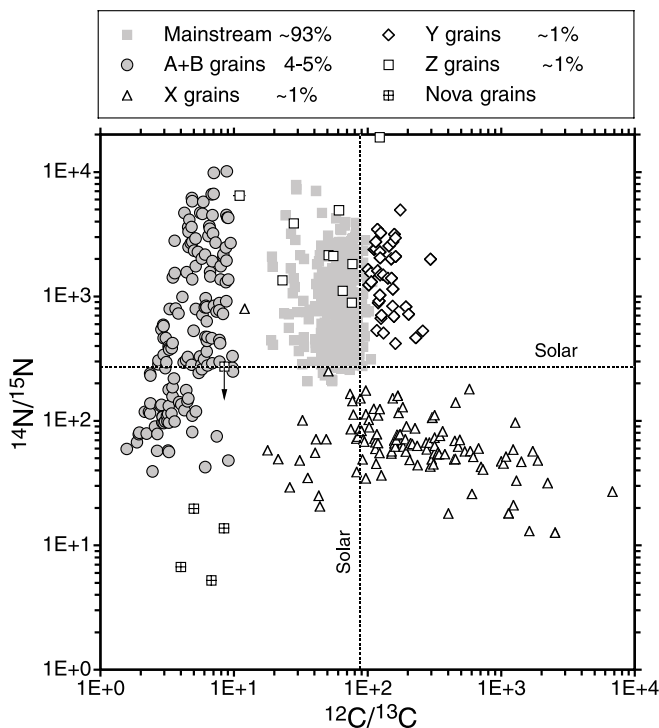


FIG. 1.—C and N isotopic ratios of different populations of presolar SiC grains. The relative grain abundances are given in the legend. Here and in Figs. 2 and 3, the numbers of grains shown from different populations do not reflect their natural abundances since grains of the minor populations were preferentially identified by ion imaging. The dotted lines indicate the solar ratios. A + B grains are defined as having  $^{12}\text{C}/^{13}\text{C} < 10$ . Many of them have higher-than-solar  $^{14}\text{N}/^{15}\text{N}$  ratios like mainstream, Y, and Z grains, but a significant fraction have lower-than-solar ratios, and the latter tend to have lower  $^{12}\text{C}/^{13}\text{C}$  ratios.

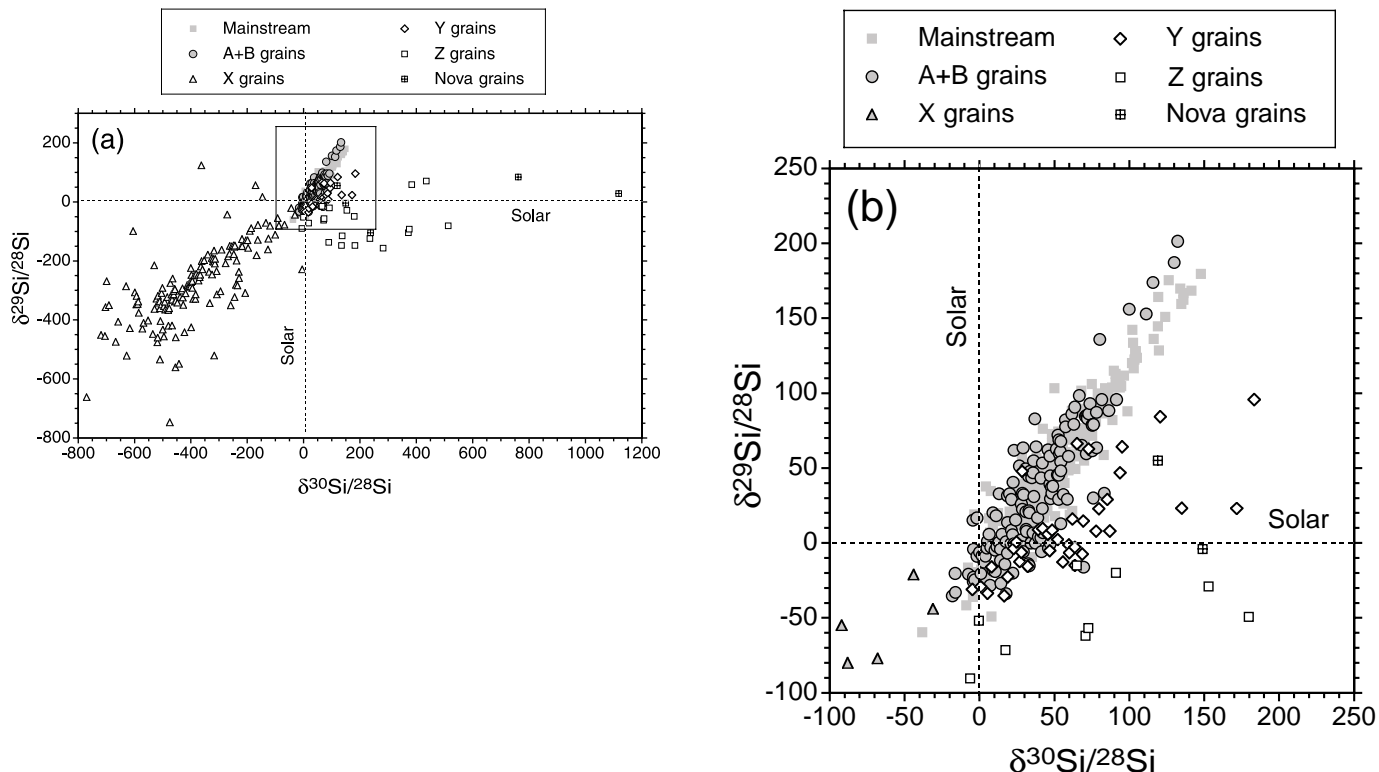


FIG. 2.—Silicon isotopic ratios of different SiC grain populations are plotted as  $\delta$  values, deviations from the solar ratios in ‰ (see § 3.3). (a) A + B grains as well as mainstream and Y grains are generally enriched in the neutron-rich Si isotopes. (b) Inset from (a). The Si of the A + B grains is similar to that of mainstream grains, suggesting that the A + B grains, as mainstream grains, formed in stars with close-to-solar metallicity.

resolution ion imaging in the ion probe (Nittler 1996; Nittler et al. 1997) as well as three A + B grains found during manual grain-by-grain analysis. We also include the isotopic ratios of the A + B grains previously measured by Hoppe et al. (1994) and the trace element data reported by Amari et al. (1995a). Preliminary reports of the isotopic data have been given by Amari et al. (1996a, 1997, 1999, 2000). In § 2 we describe the experimental procedures, and in § 3 we present the results of measurements on single grains. Possible stellar sources and the nuclear processes relevant for producing the isotopic signatures of the grains are discussed in § 4.

## 2. EXPERIMENTAL PROCEDURES

### 2.1. Sample Preparation

A procedure to extract presolar grains from meteorites is described in detail by Amari et al. (1994), and only a brief summary is given here. Approximately 83 g of the Murchison meteorite (Me 2752, Field Museum of National History) was treated alternately with HCl–HF and HCl to dissolve silicates, followed by KOH at 70°C to dissolve reactive kerogen and sulfur. The residue was further oxidized with  $\text{H}_2\text{O}_2$  to destroy sulfides, sulfates, and residual kerogen before diamond was extracted with 0.1 M  $\text{NH}_3$ . The residue was then treated with 0.5N  $\text{Na}_2\text{Cr}_2\text{O}_7$ –2N  $\text{H}_2\text{SO}_4$  to remove any reactive kerogen that had survived the previous treatment. Fractions enriched in presolar graphite were recovered by density separation with sodium polytungstate [ $\text{Na}_6(\text{H}_2\text{W}_{12}\text{O}_{40})$ ] solution before the rest of the material was treated with  $\text{HClO}_4$  to destroy chromite and any remaining carbonaceous matter. The resulting residue consisted mostly of spinel with a small amount of

SiC. After spinel was destroyed with concentrated  $\text{H}_2\text{SO}_4$  at 185°C, the residue ( $\sim 6$  ppm of the meteorite) was size sorted into nine fractions (named KJA–KJI).

The grain size fraction studied here, KJG, has a size range of 2–5  $\mu\text{m}$  in diameter. Silicon carbide comprises about 70% of KJG, oxides comprise about 20%, and unidentified Si- and Na-rich minerals account for the rest (Amari et al. 1994).

### 2.2. Ion Imaging

Ion imaging techniques, developed to search for rare types of grains, are described in detail by Nittler (1996). Grains are deposited from an isopropanol/water suspension onto a gold foil pressed onto an aluminum mount. Mass-filtered isotopic images of the grains located in a small area ( $\sim 70$  to 100  $\mu\text{m}$  diameter) are formed by the ion microprobe and recorded by a CCD camera. Isotopic ratios are then determined from the images, using image processing algorithms.

In this study, high mass resolution ( $m/\Delta m \sim 3400$ ) imaging was used to separate  $^{12}\text{CH}^-$  ions from  $^{13}\text{C}^-$  ions. This is necessary to search for X and Y grains, which have high  $^{12}\text{C}/^{13}\text{C}$  ratios, but also locates grains of type A + B with their low  $^{12}\text{C}/^{13}\text{C}$  ratios.

Two mounts, KJGM1 and KJGM4C, each of which contained about 1400 SiC grains, were imaged to search for A + B and Y grains. The results of the Y grain study have already been reported (Amari et al. 2001b). Images of  $^{12}\text{C}^-$ ,  $^{13}\text{C}^-$ ,  $^{28}\text{Si}^-$ ,  $^{29}\text{Si}^-$ , and  $^{30}\text{Si}^-$  were acquired for mount KJGM1, and images of  $^{12}\text{C}^-$ ,  $^{13}\text{C}^-$ , and  $^{28}\text{Si}^-$  for KJGM4C. A + B grain candidates were selected when the  $^{12}\text{C}/^{13}\text{C}$  ratio determined from the ion images was less than 10. Of a total of 154 candidates from the two mounts, nine

TABLE 1  
C, N, AL, AND SI ISOTOPIC RATIOS OF A AND B GRAINS

Grain	$^{12}\text{C}/^{13}\text{C}$	$^{14}\text{N}/^{15}\text{N}$	$^{26}\text{Al}/^{27}\text{Al}$ ( $\times 10^{-4}$ )	$\delta^{29}\text{Si}/^{28}\text{Si}$ (‰)	$\delta^{30}\text{Si}/^{28}\text{Si}$ (‰)
KJGM1-51-4 .....	1.96±0.02	80±2	...	21±6	31±8
KJGM1-54-5 .....	8.82±0.08	10107±2257	...	-1±6	21±8
KJGM1-61-13 .....	3.17±0.02	99±3	...	-9±5	-2±8
KJGM1-70-10 .....	4.62±0.04	4127±337	...	17±6	-2±8
KJGM1-71-11 .....	4.49±0.03	326±7	...	68±6	54±8
KJGM1-72-6 .....	6.08±0.16	43±2	...	...	...
KJGM1-86-11 .....	2.45±0.03	39±1	...	45±9	47±10
KJGM1-87-2 .....	5.57±0.04	4712±1076	...	50±6	31±8
KJGM1-88-10 .....	3.55±0.03	219±6	...	33±5	28±8
KJGM1-89-4 .....	5.37±0.04	2272±467	...	63±6	51±9
KJGM1-104-2 .....	6.13±0.05	971±157	...	-2±6	29±8
KJGM1-104-6 .....	7.40±0.06	75±3	...	-34±5	18±8
KJGM1-122-2 .....	2.90±0.02	97±4	...	-4±6	14±8
KJGM1-122-3 .....	2.98±0.02	96±2	...	-9±5	2±8
KJGM1-122-4 .....	4.25±0.04	4680±643	...	-27±7	14±9
KJGM1-130-1 .....	8.78±0.07	4514±692	...	-18±6	9±8
KJGM1-133-1 .....	4.54±0.03	3602±249	...	15±5	-4±8
KJGM1-136-1 .....	7.93±0.06	1751±219	...	30±5	48±8
KJGM1-139-3 .....	6.80±0.05	6623±1064	...	96±6	91±9
KJGM1-139-8 .....	5.87±0.05	5741±1732	...	0±6	23±8
KJGM1-149-1 .....	2.92±0.02	109±6	...	-2±5	12±8
KJGM1-152-3 .....	5.75±0.04	259±8	...	86±6	73±8
KJGM1-157-2 .....	3.87±0.03	141±4	...	1±5	13±8
KJGM1-157-3 .....	6.07±0.04	2169±147	...	33±6	20±8
KJGM1-178-2 .....	9.40±0.07	2687±269	...	30±6	76±9
KJGM1-182-2 .....	7.03±0.05	6669±904	...	0±5	37±8
KJGM1-190-7 .....	6.61±0.05	1577±187	...	82±6	57±8
KJGM1-191-2 .....	3.11±0.02	296±12	...	21±6	33±8
KJGM1-200-10 .....	4.87±0.04	110±2	...	15±6	24±8
KJGM1-211-3 .....	2.15±0.02	118±2	...	85±6	71±9
KJGM1-213-2 .....	5.69±0.04	281±5	...	79±6	63±9
KJGM1-216-2 .....	4.87±0.03	1371±69	...	91±6	64±8
KJGM1-234-2 .....	5.03±0.04	2334±183	...	93±6	74±9
KJGM1-236-4 .....	4.80±0.04	3612±481	...	62±6	46±8
KJGM1-245-1 .....	4.25±0.03	122±2	...	1±6	5±8
KJGM1-245-4 .....	1.57±0.06	59±6	...	...	...
KJGM1-252-11 .....	3.65±0.03	796±42	...	49±6	31±9
KJGM1-257-2 .....	4.83±0.04	6188±901	...	55±6	36±8
KJGM1-257-8 .....	3.46±0.03	186±8	...	32±6	19±8
KJGM1-260-1 .....	3.20±0.03	58±1	...	6±6	22±8
KJGM1-271-4 .....	3.60±0.03	1540±117	...	136±7	80±9
KJGM1-281-1 .....	3.27±0.02	384±20	...	-25±8	-3±12
KJGM1-281-5 .....	6.58±0.06	3506±407	...	69±10	53±13
KJGM1-285-1 .....	9.01±0.08	4286±585	...	-15±8	33±12
KJGM1-292-7 .....	3.27±0.03	374±17	...	-23±8	-4±12
KJGM1-301-1 .....	8.27±0.07	724±78	...	59±8	53±12
KJGM1-305-1 .....	7.27±0.06	2707±250	...	29±8	21±12
KJGM1-308-2 .....	2.66±0.02	57±2	...	65±6	68±9
KJGM1-311-2 .....	4.56±0.04	3301±593	...	33±9	13±13
KJGM1-318-2 .....	3.59±0.03	2798±527	...	54±8	54±12
KJGM1-322-11 .....	6.43±0.06	3061±478	...	-19±9	10±13
KJGM1-329-1 .....	3.25±0.02	132±6	...	7±8	42±12
KJGM1-330-2 .....	6.06±0.05	819±98	...	0±8	34±12
KJGM1-333-2 .....	7.39±0.06	756±29	...	-16±8	69±13
KJGM1-339-6 .....	4.10±0.03	991±52	...	58±8	47±12
KJGM1-341-1 .....	7.87±0.06	420±14	...	9±8	21±12
KJGM1-365-1 .....	5.15±0.04	2928±186	...	72±8	52±12
KJGM1-381-5 .....	7.04±0.05	9819±1277	...	83±8	72±12
KJGM1-382-5 .....	4.81±0.03	282±25	...	153±9	111±13
KJGM1-382-9 .....	6.53±0.05	3677±315	...	20±8	9±12
KJGM1-399-3 .....	4.75±0.03	2672±198	...	45±8	33±12
KJGM1-413-1 .....	3.23±0.02	396±16	...	-26±8	-4±12
KJGM1-425-1 .....	2.57±0.02	90±3	...	6±9	15±13
KJGM4C-9-2 .....	2.66±0.02	79±5	22.0±3.0	64±7	78±7

TABLE 1—Continued

Grain	$^{12}\text{C}/^{13}\text{C}$	$^{14}\text{N}/^{15}\text{N}$	$^{26}\text{Al}/^{27}\text{Al}$ ( $\times 10^{-4}$ )	$\delta^{29}\text{Si}/^{28}\text{Si}$ (‰)	$\delta^{30}\text{Si}/^{28}\text{Si}$ (‰)
KJGM4C-39-1 .....	2.71 ± 0.01	286 ± 8	19.4 ± 0.5	37 ± 3	48 ± 4
KJGM4C-42-8 .....	3.30 ± 0.02	793 ± 70	...	...	...
KJGM4C-45-1 .....	4.37 ± 0.03	176 ± 9	0.8 ± 0.3	-20 ± 5	1 ± 6
KJGM4C-62-2 .....	7.76 ± 0.08	776 ± 166	19.1 ± 3.0	79 ± 15	76 ± 17
KJGM4C-62-3 .....	5.17 ± 0.03	794 ± 124	30.7 ± 4.3	33 ± 5	48 ± 5
KJGM4C-65-4 .....	2.71 ± 0.01	305 ± 23	17.0 ± 4.3	23 ± 3	42 ± 4
KJGM4C-66-8 .....	3.21 ± 0.02	114 ± 4	58.0 ± 1.7	88 ± 4	86 ± 4
KJGM4C-77-3 .....	5.73 ± 0.03	2014 ± 200	...	...	...
KJGM4C-79-2 .....	2.97 ± 0.01	463 ± 44	0.4 ± 0.4	86 ± 5	62 ± 5
KJGM4C-86-3 .....	3.59 ± 0.02	99 ± 2	> 3.3	-4 ± 7	-4 ± 8
KJGM4C-87-4 .....	7.77 ± 0.04	299 ± 10	...	...	...
KJGM4C-97-2 .....	3.04 ± 0.02	99 ± 3	30.5 ± 1.0	6 ± 6	6 ± 6
KJGM4C-98-3 .....	7.07 ± 0.05	840 ± 204	10.3 ± 3.7	85 ± 5	72 ± 6
KJGM4C-99-2 .....	2.37 ± 0.01	138 ± 7	50.3 ± 2.0	23 ± 3	29 ± 4
KJGM4C-100-4 .....	4.42 ± 0.03	1567 ± 420	11.5 ± 2.7	-3 ± 5	46 ± 6
KJGM4C-104-4 .....	8.31 ± 0.05	2081 ± 220	2.7 ± 0.2	29 ± 4	53 ± 5
KJGM4C-111-6 .....	2.35 ± 0.02	240 ± 15	2.8 ± 1.3	79 ± 14	75 ± 15
KJGM4C-113-2 .....	2.35 ± 0.01	115 ± 2	33.4 ± 0.7	64 ± 6	29 ± 6
KJGM4C-115-9 .....	3.46 ± 0.02	157 ± 4	7.7 ± 0.4	29 ± 6	59 ± 6
KJGM4C-119-5 .....	1.88 ± 0.01	67 ± 1	20.5 ± 0.8	20 ± 5	33 ± 6
KJGM4C-126-5 .....	4.87 ± 0.02	2742 ± 198	> 28.6	61 ± 3	54 ± 3
KJGM4C-128-5 .....	6.15 ± 0.03	842 ± 92	2.8 ± 3.0	4 ± 4	39 ± 4
KJGM4C-130-4 .....	2.95 ± 0.01	591 ± 68	...	87 ± 4	78 ± 5
KJGM4C-135-5 .....	6.86 ± 0.05	1919 ± 164	37.3 ± 0.9	-13 ± 3	3 ± 4
KJGM4C-138-1 .....	6.89 ± 0.04	4487 ± 805	13.3 ± 2.6	-6 ± 4	29 ± 5
KJGM4C-166-6 .....	6.23 ± 0.04	819 ± 135	0.7 ± 0.2	4 ± 5	41 ± 6
KJGM4C-184-1 .....	4.87 ± 0.04	81 ± 3	43.6 ± 3.6	45 ± 7	53 ± 8
KJGM4C-188-4 .....	3.48 ± 0.02	1422 ± 170	24.5 ± 1.1	26 ± 7	28 ± 7
KJGM4C-204-1 .....	8.76 ± 0.05	1940 ± 186	2.7 ± 0.4	7 ± 3	36 ± 4
KJGM4C-205-1 .....	5.55 ± 0.03	329 ± 34	> 0.6	-20 ± 4	22 ± 5
KJGM4C-224-10 .....	4.18 ± 0.02	294 ± 13	11.5 ± 1.0	32 ± 4	56 ± 4
KJGM4C-225-9 .....	8.70 ± 0.10	2468 ± 538	15.4 ± 2.1	45 ± 15	52 ± 16
KJGM4C-240-1 .....	4.57 ± 0.02	2491 ± 245	...	...	...
KJGM4C-246-3 .....	2.36 ± 0.01	231 ± 8	32.5 ± 1.1	-28 ± 3	7 ± 3
KJGM4C-250-3 .....	6.66 ± 0.04	1452 ± 155	28.0 ± 1.7	7 ± 4	46 ± 5
KJGM4C-256-1 .....	6.94 ± 0.04	3205 ± 803	24.3 ± 13.8	-1 ± 3	47 ± 3
KJGM4C-260-8 .....	4.98 ± 0.04	529 ± 90	> 0.6	51 ± 9	27 ± 10
KJGM4C-262-1 .....	5.80 ± 0.04	711 ± 124	> 0.3	43 ± 5	41 ± 5
KJGM4C-262-3 .....	2.22 ± 0.01	79 ± 2	50.1 ± 1.3	17 ± 4	39 ± 5
KJGM4C-278-2 .....	3.26 ± 0.02	56 ± 1	37.3 ± 1.2	13 ± 7	54 ± 7
KJGM4C-281-3 .....	4.86 ± 0.02	5838 ± 586	11.6 ± 1.0	59 ± 8	71 ± 8
KJGM4C-283-3 .....	2.86 ± 0.02	543 ± 99	15.3 ± 5.1	79 ± 7	75 ± 7
KJGM4C-284-5 .....	5.17 ± 0.03	119 ± 4	...	...	...
KJGM4C-287-3 .....	7.92 ± 0.05	1367 ± 101	> 1.8	38 ± 4	49 ± 4
KJGM4C-296-3 .....	8.31 ± 0.10	2171 ± 279	0.4 ± 0.3	14 ± 6	19 ± 6
KJGM4C-305-3 .....	6.24 ± 0.04	632 ± 99	...	39 ± 5	47 ± 5
KJGM4C-311-7 .....	5.16 ± 0.06	1755 ± 233	> 3.0	41 ± 11	22 ± 12
KJGM4C-312-6 .....	8.68 ± 0.06	1300 ± 127	> 1.3	174 ± 5	116 ± 5
KJGM4C-313-9 .....	3.26 ± 0.02	97 ± 2	53.3 ± 1.9	-20 ± 6	-16 ± 7
KJGM4C-314-3 .....	4.04 ± 0.02	136 ± 3	9.9 ± 1.2	8 ± 4	31 ± 4
KJGM4C-315-2 .....	3.41 ± 0.02	114 ± 3	23.0 ± 0.7	-5 ± 3	10 ± 4
KJGM4C-316-29 .....	3.83 ± 0.04	729 ± 87	42.3 ± 2.2	58 ± 7	59 ± 7
KJGM4C-316-8 .....	2.31 ± 0.01	118 ± 5	28.7 ± 3.6	2 ± 4	28 ± 4
KJGM4C-325-4 .....	9.06 ± 0.09	48 ± 1	> 2.9	33 ± 6	83 ± 6
KJGM4C-338-5 .....	3.15 ± 0.02	109 ± 4	36.7 ± 2.6	-7 ± 6	19 ± 6
KJGM4C-352-3 .....	6.87 ± 0.04	290 ± 49	4.9 ± 1.5	83 ± 5	37 ± 6
KJGM4C-355-3 .....	3.42 ± 0.02	382 ± 35	23.1 ± 4.0	-14 ± 5	17 ± 6
KJGP1-61-2 .....	4.38 ± 0.04	308 ± 20	...	156 ± 6	100 ± 11
KJGP1-289-1 .....	3.46 ± 0.03	422 ± 58	...	-9 ± 11	4 ± 14
KJGP1-342-1 .....	9.03 ± 0.10	1364 ± 175	...	62 ± 11	23 ± 13
KJG2-154 <sup>a</sup> .....	8.89 ± 0.07	4303 ± 921	6.3 ± 0.7	-12 ± 7	14 ± 7
KJG2-243 <sup>a</sup> .....	5.80 ± 0.04	4612 ± 479	35.0 ± 1.0	47 ± 4	36 ± 5
KJG2-1412 <sup>a</sup> .....	9.80 ± 0.08	249 ± 26	...	98 ± 4	66 ± 5
KJG2-2311 <sup>a</sup> .....	8.74 ± 0.08	917 ± 114	8.7 ± 1.3	96 ± 4	82 ± 4
KJH4-222 <sup>a</sup> .....	4.35 ± 0.05	...	21.4 ± 3.4	187 ± 5	130 ± 6
KJH5-042 <sup>a</sup> .....	2.92 ± 0.03	107 ± 5	47.6 ± 6.0	31 ± 4	36 ± 3

TABLE 1—Continued

Grain	$^{12}\text{C}/^{13}\text{C}$	$^{14}\text{N}/^{15}\text{N}$	$^{26}\text{Al}/^{27}\text{Al}$ ( $\times 10^{-4}$ )	$\delta^{29}\text{Si}/^{28}\text{Si}$ (‰)	$\delta^{30}\text{Si}/^{28}\text{Si}$ (‰)
KJH5-121 <sup>a</sup> .....	5.97 ± 0.07	313 ± 34	...	1 ± 5	18 ± 3
KJH5-631 <sup>a</sup> .....	6.82 ± 0.07	462 ± 41	...	48 ± 5	54 ± 3
KJH5-741 <sup>a</sup> .....	2.97 ± 0.03	577 ± 86	59.1 ± 15.2	-3 ± 4	5 ± 3
KJH5-m131 <sup>a</sup> .....	2.97 ± 0.03	340 ± 32	11.3 ± 1.7	77 ± 4	58 ± 3
KJH6-031 <sup>a</sup> .....	3.08 ± 0.03	464 ± 55	17.6 ± 3.7	84 ± 7	72 ± 12
KJH7-552 <sup>a</sup> .....	6.24 ± 0.04	360 ± 51	...	62 ± 5	76 ± 5
KJH7-LL11 <sup>a</sup> .....	3.24 ± 0.03	178 ± 10	67.8 ± 8.1	-3 ± 4	8 ± 4
KJH8-151 <sup>a</sup> .....	1.94 ± 0.02	78 ± 4	18.6 ± 1.5	9 ± 5	31 ± 5
KJH8-241 <sup>a</sup> .....	2.83 ± 0.03	132 ± 19	87.9 ± 6.7	-21 ± 3	-7 ± 3
KJH9-523 <sup>a</sup> .....	6.33 ± 0.15	472 ± 40	...	-6 ± 24	42 ± 24
KJH9-CL16 <sup>a</sup> .....	4.55 ± 0.03	151 ± 6	...	-33 ± 5	-16 ± 8
KJH10-171 <sup>a</sup> .....	6.10 ± 0.04	475 ± 39	...	-14 ± 4	32 ± 8
KJH10-272 <sup>a</sup> .....	7.74 ± 0.05	446 ± 31	12.8 ± 2.5	201 ± 4	132 ± 8
KJH10-274 <sup>a</sup> .....	2.87 ± 0.02	134 ± 5	43.5 ± 2.8	64 ± 3	38 ± 7
KJH10-461 <sup>a</sup> .....	9.69 ± 0.07	267 ± 27	...	44 ± 3	35 ± 7
KJH10-553 <sup>a</sup> .....	3.06 ± 0.02	265 ± 23	...	-6 ± 4	0 ± 8
KJH10-561 <sup>a</sup> .....	9.74 ± 0.08	330 ± 40	...	32 ± 3	30 ± 8
KJH10-741 <sup>a</sup> .....	4.47 ± 0.03	143 ± 8	46.8 ± 4.1	-35 ± 3	-18 ± 8
KJH10-LR12 <sup>a</sup> .....	6.32 ± 0.04	279 ± 11	...	53 ± 4	42 ± 8
KJH10-LR41 <sup>a</sup> .....	5.45 ± 0.05	243 ± 17	3.0 ± 0.5	18 ± 5	11 ± 9
KJH10-m161 <sup>a</sup> .....	6.26 ± 0.05	441 ± 27	1.8 ± 0.6	48 ± 6	34 ± 9
KJH10-UR11 <sup>a</sup> .....	7.75 ± 0.06	882 ± 148	...	...	...

NOTE.—Table 1 is also available in machine-readable form in the electronic edition of the *Astrophysical Journal*.

<sup>a</sup> Data from Hoppe et al. 1994.

TABLE 2  
TITANIUM ISOTOPIC RATIOS OF A AND B GRAINS

Grain	$\delta^{46}\text{Ti}/^{48}\text{Ti}$ (‰)	$\delta^{47}\text{Ti}/^{48}\text{Ti}$ (‰)	$\delta^{49}\text{Ti}/^{48}\text{Ti}$ (‰)	$\delta^{50}\text{Ti}/^{48}\text{Ti}$ (‰)
KJGM4C-9-2 <sup>a</sup> .....	106 ± 30	58 ± 29	85 ± 35	275 ± 43
KJGM4C-39-1 <sup>a</sup> .....	127 ± 29	63 ± 29	8 ± 33	-48 ± 35
KJGM4C-62-3 .....	62 ± 46	67 ± 48	36 ± 56	38 ± 62
KJGM4C-65-4 .....	48 ± 24	26 ± 24	11 ± 28	28 ± 45
KJGM4C-66-8 <sup>a</sup> .....	16 ± 49	-16 ± 49	13 ± 59	257 ± 75
KJGM4C-98-3 <sup>a</sup> .....	133 ± 27	80 ± 27	95 ± 32	132 ± 36
KJGM4C-99-2 .....	39 ± 33	-16 ± 33	89 ± 42	-64 ± 43
KJGM4C-100-4 .....	-41 ± 49	-23 ± 52	-98 ± 58	1 ± 69
KJGM4C-104-4 <sup>a</sup> .....	14 ± 20	-8 ± 20	6 ± 24	117 ± 29
KJGM4C-111-6 .....	-17 ± 43	13 ± 45	54 ± 55	36 ± 62
KJGM4C-115-9 .....	4 ± 32	32 ± 33	13 ± 39	-12 ± 43
KJGM4C-128-5 .....	50 ± 87	-100 ± 81	59 ± 107	49 ± 141
KJGM4C-135-5 <sup>a</sup> .....	152 ± 37	180 ± 38	42 ± 42	2 ± 46
KJGM4C-138-1 .....	-14 ± 31	-15 ± 32	33 ± 39	7 ± 42
KJGM4C-184-1 .....	445 ± 244	390 ± 244	296 ± 272	396 ± 314
KJGM4C-204-1 .....	52 ± 28	-6 ± 28	55 ± 34	2 ± 37
KJGM4C-224-10 <sup>a</sup> .....	47 ± 22	28 ± 22	62 ± 27	143 ± 33
KJGM4C-246-3 .....	-19 ± 34	-5 ± 35	-33 ± 41	28 ± 48
KJGM4C-256-1 .....	-10 ± 39	-60 ± 39	97 ± 51	65 ± 56
KJGM4C-262-1 <sup>a</sup> .....	-29 ± 30	29 ± 32	-25 ± 37	-104 ± 39
KJGM4C-262-3 .....	-13 ± 63	108 ± 71	67 ± 82	10 ± 87
KJGM4C-281-3 .....	210 ± 203	65 ± 192	194 ± 244	-4 ± 311
KJGM4C-287-3 <sup>a</sup> .....	24 ± 35	-52 ± 34	22 ± 42	155 ± 51
KJGM4C-314-3 <sup>a</sup> .....	100 ± 37	56 ± 36	234 ± 48	216 ± 52
KJGM4C-315-2 .....	17 ± 32	54 ± 33	-13 ± 38	-6 ± 54
KJGM4C-316-29 .....	13 ± 50	-56 ± 49	-57 ± 58	-85 ± 63
KJGM4C-316-8 .....	12 ± 57	28 ± 60	116 ± 75	-136 ± 71
KJGM4C-355-3 <sup>a</sup> .....	27 ± 40	-8 ± 40	31 ± 48	135 ± 57
KJH4-222 <sup>a, b</sup> .....	163 ± 20	52 ± 14	118 ± 16	145 ± 30
KJH10-272 <sup>a, b</sup> .....	138 ± 10	59 ± 9	92 ± 21	185 ± 33

<sup>a</sup> Titanium isotopic patterns of these grains are shown in Fig. 6.

<sup>b</sup> Data from Hoppe et al. 1994.

grains turned out to be aggregates of more than two grains. The remaining 145 candidate grains were analyzed individually in the ion probe under standard single-grain analysis conditions.

### 2.3. High Mass Resolution Isotopic Analysis

Techniques of high mass resolution isotopic analysis have been described by Zinner, Tang, & Anders (1989). C and N isotopic analyses confirmed 63 grains on KJGM1 and 58 grains on KJGM4 to be A+B grains (Table 1). We also include three A+B grains from the KJGP1 mount. This mount was imaged in a search for X grains in order to study them by RIMS (Pellin et al. 2000a). Subsequently, when non-X grains on the mount were randomly selected and had their C, N, and Si isotopic ratios measured for comparison, three A+B grains were found.

Tables 1 and 2 give the C, N, Al, Si, and Ti isotopic ratios of A+B grains including those measured by Hoppe et al. (1994). Altogether, C and N isotopic ratios were measured in 151 grains but no N isotopic ratio in grain KJH4-222. However, other isotopic ratios of the grain indicate that it is an A+B and not a nova grain.  $^{26}\text{Al}/^{27}\text{Al}$  ratios were inferred from  $^{26}\text{Mg}$  excesses in 59 grains, and in an additional 11 grains only lower limits of  $^{26}\text{Al}/^{27}\text{Al}$  could be obtained as a result of the presence of  $^{27}\text{Al}^+$  signals from nearby Al-rich oxide grains. A total of 144 grains had their Si isotopic ratios measured and 30 grains their Ti isotopic ratios (Table 2).

## 3. RESULTS

### 3.1. Carbon and Nitrogen Isotopic Ratios

C and N isotopic ratios of A+B grains are plotted in Figure 1 together with those of other SiC populations. We note that in Figures 1, 2, and 3 the numbers of the grains from different populations do not reflect their natural abundances among all presolar SiC grains because grains of the minor populations were selectively located by ion imaging (e.g., see Nittler et al. 1995; Hoppe et al 1996a; Amari et al 2001b).

The  $^{12}\text{C}/^{13}\text{C}$  ratios of the A+B grains range from 1.6 to 9.8, the  $^{14}\text{N}/^{15}\text{N}$  ratios from 39 to 10,100. Although high  $^{14}\text{N}/^{15}\text{N}$  ratios close to 10,000 are also observed in mainstream grains, a marked difference between the two populations is that the  $^{14}\text{N}/^{15}\text{N}$  ratios of the A+B grains extend to much lower values and that there are many more grains with subsolar  $^{14}\text{N}/^{15}\text{N}$  ratios than among the mainstream grains (34% of the A+B grains, compared to 3% of mainstream grains with the same size range as the A+B grains). For the A+B grains C and N isotopic ratios are correlated such that grains with low  $^{12}\text{C}/^{13}\text{C}$  ratios have, on average, lower  $^{14}\text{N}/^{15}\text{N}$  ratios.

Nova grains also have low  $^{12}\text{C}/^{13}\text{C}$  and even lower  $^{14}\text{N}/^{15}\text{N}$  ratios. However, their other isotopic features differ markedly from those of A+B grains, making them a distinct population. These grains are discussed in detail by Amari et al. (2001a).

### 3.2. Aluminum Isotopic Ratios

The initial  $^{26}\text{Al}/^{27}\text{Al}$  ratios, inferred from  $^{26}\text{Mg}$  excesses and Al/Mg ratios, of many A+B grains range up to  $10^{-2}$  (Fig. 3). These are lower on average than those of X grains, but significantly higher than those of mainstream and Y grains, most of which have ratios smaller than  $10^{-3}$ . An isotopic correlation is also observed for the  $^{26}\text{Al}/^{27}\text{Al}$

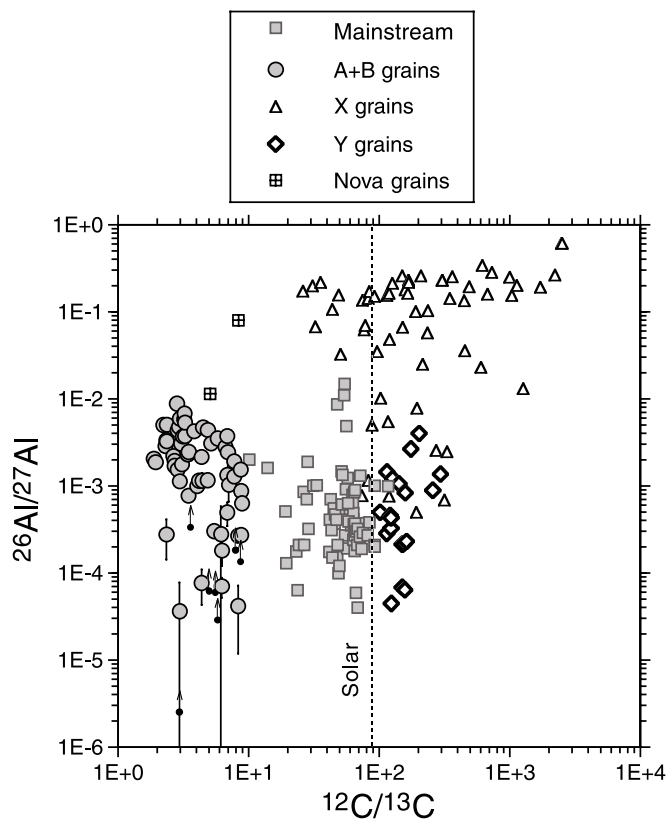


FIG. 3.— $^{26}\text{Al}/^{27}\text{Al}$  ratios inferred from  $^{26}\text{Mg}$  excesses are plotted against C isotopic ratios for SiC grains of different populations. No Mg-Al measurements have been performed on Z grains. Error bars in this and subsequent figures are  $1\sigma$ . Arrows on some points indicate lower limits of the ratios because of the presence of a  $^{27}\text{Al}^+$  signal from Al-rich oxide grains in the proximity of the analyzed grains. Although the  $^{26}\text{Al}/^{27}\text{Al}$  ratios of the A+B grains cover the same range as those of the mainstream grains, on average, the ratios of the A+B grains are higher than those of the mainstream grains. The negative correlation between  $^{26}\text{Al}/^{27}\text{Al}$  and  $^{12}\text{C}/^{13}\text{C}$  ratios extends to the A+B grains themselves: grains with lower  $^{12}\text{C}/^{13}\text{C}$  ratios have higher  $^{26}\text{Al}/^{27}\text{Al}$  ratios.

ratios: grains with lower  $^{12}\text{C}/^{13}\text{C}$  ratios (thus lower  $^{14}\text{N}/^{15}\text{N}$  ratios) tend to have higher  $^{26}\text{Al}/^{27}\text{Al}$  ratios.

### 3.3. Silicon Isotopic Ratios

The Si isotopic ratios in Figure 2 are plotted as  $\delta$ -values, deviations in parts per thousand (‰) from the solar ratios  $^{29}\text{Si}/^{28}\text{Si}_\odot = 0.0506331$  and  $^{30}\text{Si}/^{28}\text{Si}_\odot = 0.0334744$  ( $\delta^i\text{Si}/^{28}\text{Si} \equiv [({}^i\text{Si}/^{28}\text{Si})_{\text{grain}}/({}^i\text{Si}/^{28}\text{Si})_{\text{solar}} - 1]1000$ ). Like the mainstream grains, most A+B grains are enriched in the neutron-rich Si isotopes. Their  $\delta^{29}\text{Si}/^{28}\text{Si}$  values range from  $-35\text{‰}$  to  $201\text{‰}$  and the  $\delta^{30}\text{Si}/^{28}\text{Si}$  values from  $-18\text{‰}$  to  $132\text{‰}$ . We obtain the following averages for the 144 A+B grains:  $\delta^{29}\text{Si}/^{28}\text{Si}_{\text{weighted mean}} = 30.7$ ,  $\delta^{29}\text{Si}/^{28}\text{Si}_{\text{std. dev.}} = 45.0$ ,  $\delta^{30}\text{Si}/^{28}\text{Si}_{\text{weighted mean}} = 38.1$ ,  $\delta^{30}\text{Si}/^{28}\text{Si}_{\text{std. dev.}} = 29.0$ . Lugaro et al. (1999) calculated the averages of mainstream grains:  $\delta^{29}\text{Si}/^{28}\text{Si}_{\text{weighted mean}} = 50.4$ ,  $\delta^{29}\text{Si}/^{28}\text{Si}_{\text{std. dev.}} = 42.7$ ,  $\delta^{30}\text{Si}/^{28}\text{Si}_{\text{weighted mean}} = 52.0$ ,  $\delta^{30}\text{Si}/^{28}\text{Si}_{\text{std. dev.}} = 30.6$ . A+B grains have, on average, slightly lower  $^{29}\text{Si}/^{28}\text{Si}$  and  $^{30}\text{Si}/^{28}\text{Si}$  ratios than mainstream grains with a very similar spread in the ratios.

### 3.4. Titanium Isotopic Ratios

In Figures 4 and 5, Ti and Si isotopic ratios of the A+B grains are plotted together with those of the mainstream grains measured by Hoppe et al. (1994) and Alexander &

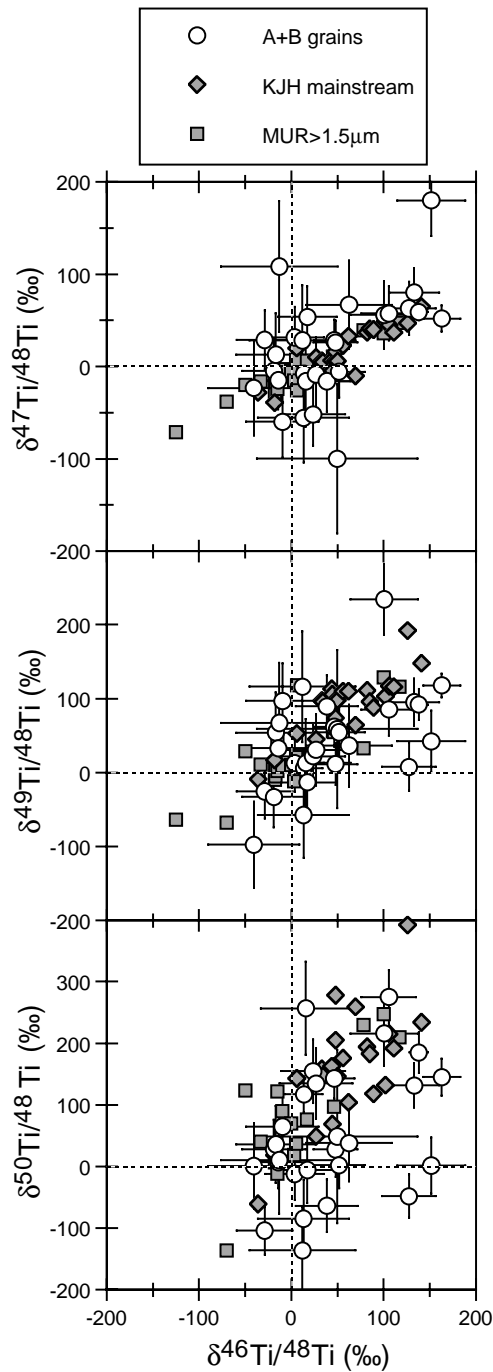


FIG. 4.—Titanium isotopic ratios (expressed as  $\delta$  values) of A + B grains are compared to those of mainstream grains of the KJH size fraction (Hoppe et al. 1994) and of Murchison mainstream grains analyzed by Alexander & Nittler (1999). Error bars of the mainstream grains are not plotted in this and the following figure to avoid clutter. The Ti isotopic distribution of the A + B grains is not clearly distinct from that of the mainstream grains.

Nittler (1999). Our Ti isotopic ratios are listed in Table 2 as well as those by Hoppe et al. (1994), again as  $\delta$ -values ( $\delta^i\text{Ti}/^{48}\text{Ti} \equiv [({}^i\text{Ti}/^{48}\text{Ti})_{\text{grain}}/({}^i\text{Ti}/^{48}\text{Ti})_{\text{solar}} - 1]1000$ ). It should be noted that the mainstream grains in the figures are not a representative sample of the population: Hoppe et al. (1994) preferentially selected grains with high  $\delta^{29}\text{Si}/^{28}\text{Si}$  and  $\delta^{30}\text{Si}/^{28}\text{Si}$  values, whereas Alexander & Nittler (1999) chose grains with high Ti concentrations. Even then the

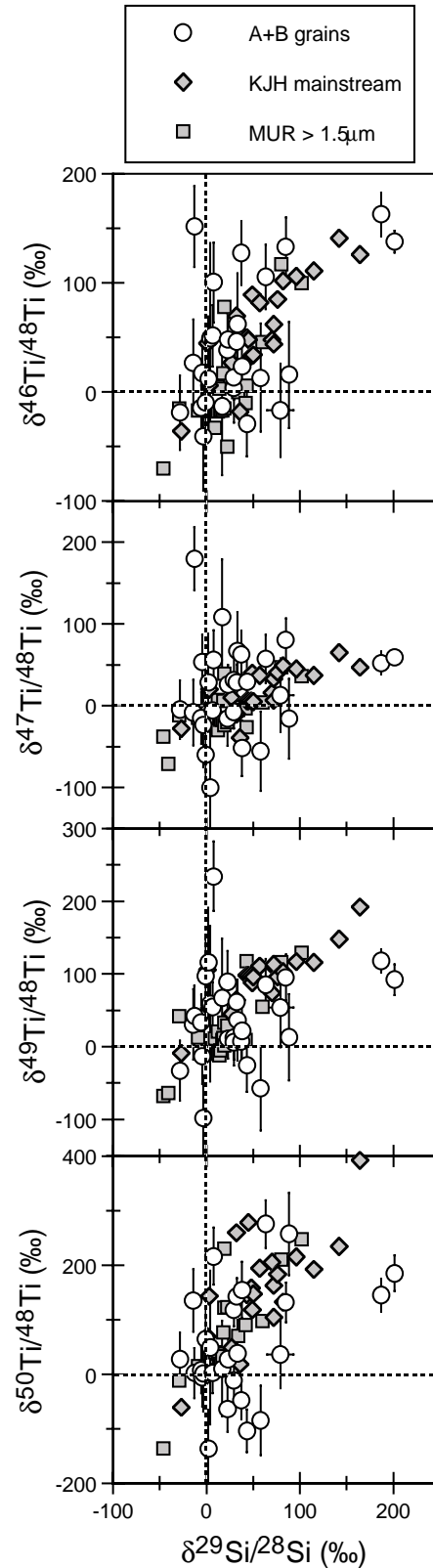


FIG. 5.—Titanium isotopic ratios of A + B grains and mainstream grains are plotted against their  $^{29}\text{Si}/^{28}\text{Si}$  ratios. Most A + B grains fall in the same region as the mainstream grains. Two KJH grains (KJH4-222 and KJH10-272) have the highest  $\delta^{29}\text{Si}/^{28}\text{Si}$  values among the A + B grains, but their  $\delta^{49}\text{Ti}/^{48}\text{Ti}$  and  $\delta^{50}\text{Ti}/^{48}\text{Ti}$  values do not follow the general correlation exhibited by most other grains.

distribution of the Ti isotopic ratios of the A + B grains is similar to that of the mainstream grains except for grain KJGM4C-135-5, which has large  $^{46}\text{Ti}$  and  $^{47}\text{Ti}$  excesses but essentially normal  $^{49}\text{Ti}/^{48}\text{Ti}$ ,  $^{50}\text{Ti}/^{48}\text{Ti}$ , and Si isotopic ratios (see also Fig. 6). Two grains (KJGM4C-184-1 and KJGM4C-281-3) with very large errors are not plotted in Figures 4 and 5.

It has previously been observed that in mainstream grains the Ti isotopic ratios correlate with the Si ratios (Fig. 5) (Hoppe et al. 1994). Again, many of the A + B grains cluster within the same ranges as the mainstream grains. Because of the large errors, however, it is not clear whether there are any systematic differences between the A + B and the mainstream grains. KJH4-222 and KJH10-272 have the highest  $\delta^{29}\text{Si}/^{28}\text{Si}$  values. Whereas in the  $\delta^{46}\text{Ti}/^{48}\text{Ti}$  and

$\delta^{47}\text{Ti}/^{48}\text{Ti}$  versus  $\delta^{29}\text{Si}/^{28}\text{Si}$  diagrams they plot along the trend of the mainstream grains, they lie outside of this trend in the  $\delta^{49}\text{Ti}/^{48}\text{Ti}$  and  $\delta^{50}\text{Ti}/^{48}\text{Ti}$  versus  $\delta^{29}\text{Si}/^{28}\text{Si}$  diagrams.

The Ti isotopic patterns of the 13 A + B grains that deviate from solar by more than  $2\sigma$  in at least one isotopic ratio are plotted in Fig. 6. Six grains show excesses in all the isotopes relative to  $^{48}\text{Ti}$ , having a V-shaped pattern. Four grains have only  $^{50}\text{Ti}$  excesses within  $2\sigma$  errors. Two grains are enriched in  $^{46}\text{Ti}$  and  $^{47}\text{Ti}$ . One grain shows a  $^{50}\text{Ti}$  deficit with all the other Ti isotopic ratios being solar. This is in contrast to the mainstream grains measured by Hoppe et al. (1994) where a majority, 19 out of 22 mainstream grains, show a V-shaped pattern. On the other hand, only three out of 10 grains analyzed by Alexander & Nittler (1999) show

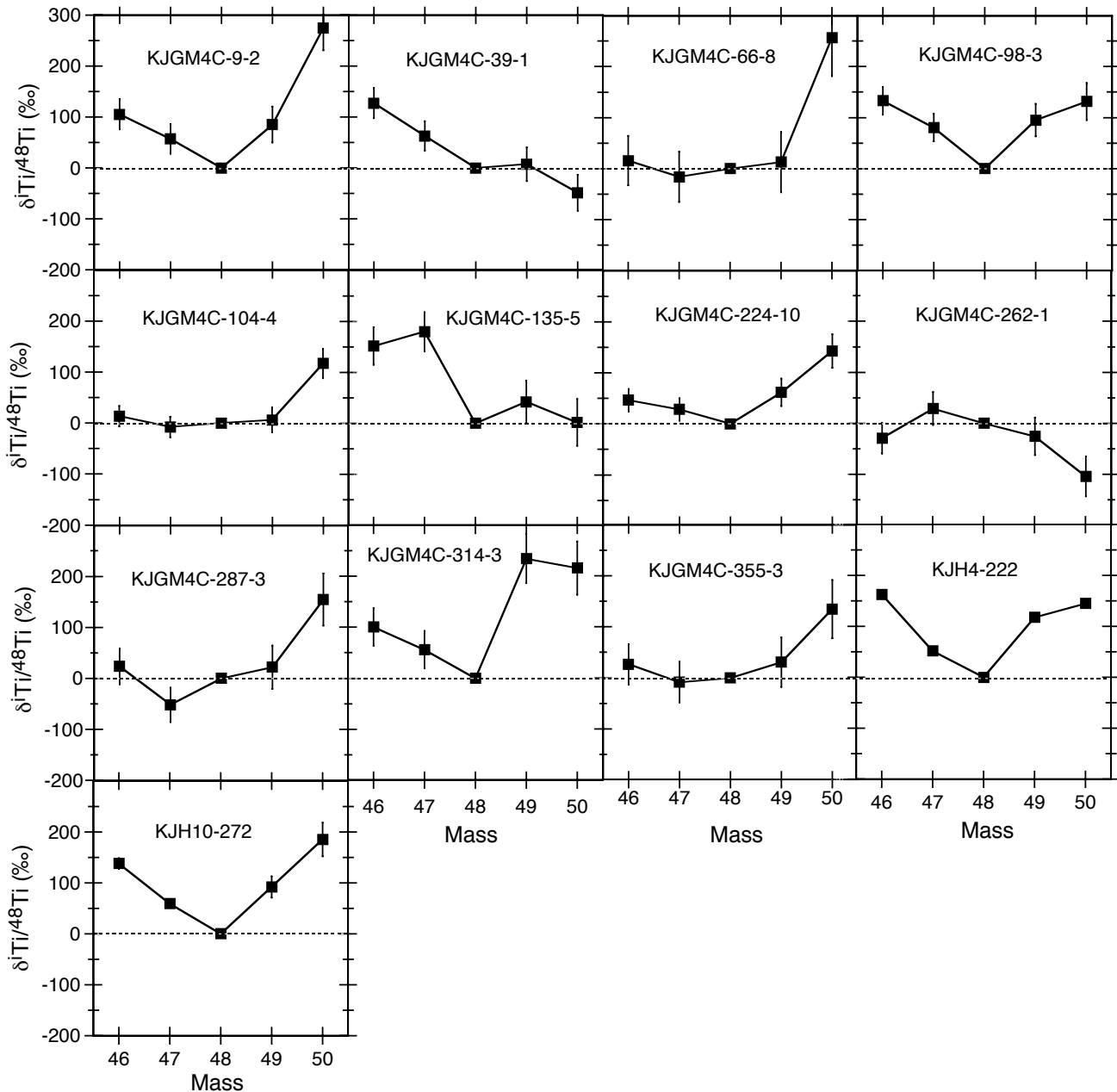


FIG. 6.—Titanium isotopic patterns of the A + B grains that have isotopic anomalies greater than  $2\sigma$  in at least one isotopic ratio. Six grains show excesses in all the isotopes relative to  $^{48}\text{Ti}$ ; four grains have only  $^{50}\text{Ti}$  excesses; two grains are enriched in the light isotopes,  $^{46}\text{Ti}$  and  $^{47}\text{Ti}$ ; one grain shows a  $^{50}\text{Ti}$  deficit.

the V-shaped pattern. Since Hoppe et al. (1994) have focused on the mainstream grains with large  $^{29}\text{Si}$  and  $^{30}\text{Si}$  excesses for Ti isotopic analyses, one may wonder whether such a high occurrence of grains with the V-shaped pattern is a result of their grain selection. However,  $\delta^{29}\text{Si}/^{28}\text{Si}$  values of such mainstream grains range from 27‰ to 164‰ and are not much different from those of the six A + B grains with a V-shaped pattern (8‰–201‰). This apparent difference in the titanium isotopic patterns in the populations of mainstream and A + B grains is a puzzle.

### 3.5. Trace Element Abundances

We have not measured trace element abundances of A + B grains from the KJG fraction because there was hardly any material left after Ti isotopic analysis. Amari et al. (1995a) reported trace element abundances of 21 A + B grains from the SiC size fraction KJH (3–6  $\mu\text{m}$ ). Except for one grain that was unclassified, the grains have been classified into several groups according to their trace element patterns (Fig. 7). In this figure, the abundances of the elements are normalized with respect to Si and solar abundances (Anders & Grevesse 1989). Seven grains show deficiencies in Sr and a relatively flat pattern in the heavy elements (Fig. 7a). Three grains also have a flat pattern from

Ti to Y with enrichments in Ba (Fig. 7b). Four grains with depletions are plotted in Figure 7c. Two of them (D1 in the legend) are depleted in essentially all the elements (except for Nb) relative to Si, while the other two (D2) are moderately enriched in Y and Ba compared to the other elements. Finally, six grains are depleted in Sr but enriched in Y and Zr (Fig. 7d). Three of them (E1) are also enriched in Ba, whereas the other three (E3) have normal Ba or a Ba depletion.

The trace element abundances measured in the A + B grains show a range of patterns. The abundances of various trace elements in SiC are determined by both the concentrations of these elements in the stellar atmosphere from which the grains condensed and the condensation behavior of the elements (primarily as a function of temperature). Lodders & Fegley (1995) have calculated the condensation sequence of minerals from a C-rich ( $\text{C} > \text{O}$ ) atmosphere by assuming varying enrichments of the *s*-process elements (solar to 10 times solar). These authors also assumed varying depletions of highly refractory elements under the assumption that these elements had condensed into other phases before the onset of SiC condensation. Under these assumptions, they could successfully reproduce the patterns shown in Figure 7. The Flat 1 pattern (Fig. 7a) (named Class I pattern in

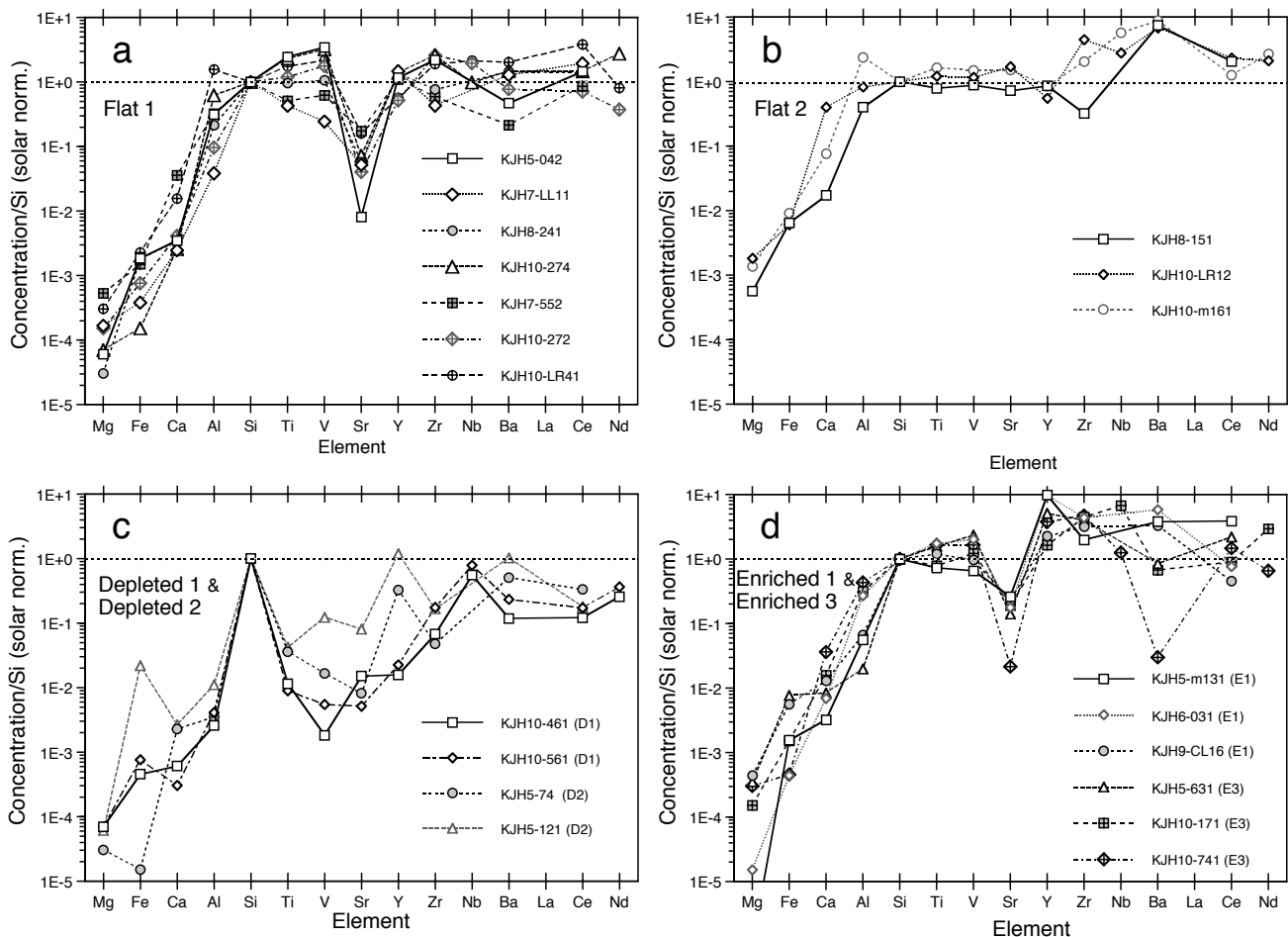


FIG. 7.—Trace element abundance patterns of the A + B grains measured by Amari et al. (1995a). The abundances are normalized to Si and to the solar abundance (dotted lines). (a) Seven grains show deficiencies in Sr with relatively flat patterns in the heavy elements. (b) Three grains have a flat pattern in the elements from Al on with Ba enrichments. (c) Two grains (D1) are depleted in all elements, and the other two (D2), while depleted, are relatively enriched in Y and Ba. (d) All six grains are depleted in Sr but enriched in Y and Zr, and three of them (E1) have Ba excesses and the other three (E3) normal Ba and a Ba depletion. Condensation calculations by Lodders & Fegley (1995) indicate that the grains in (a) formed in an atmosphere with no *s*-process enhancement, whereas the grains in (b)–(d) formed from atmospheres with various degrees of *s*-process enrichments.

Table 8 of Lodders & Fegley 1995) is obtained under the assumption that SiC condenses from an atmosphere with solar *s*-process abundances and that no highly refractory elements have previously been removed from the atmosphere. On the other hand, the other patterns (Figs. 7*b*–7*d*) can be explained with *s*-process enrichments of 3–5 times solar and various degrees of depletion of highly refractory elements: the Flat 2 pattern (Fig. 7*b*) (Class IV) with 3 times solar *s*-process enrichments and removal of 65% of high-temperature elements before SiC condensation, the E1 pattern (Class III, 9*f*) with threefold enrichments and 46% removal, the E3 pattern (Class III, 9*e*) with fourfold enrichments and no removal, the D1 pattern (Class III, 1*h*) with threefold enrichments and 92% removal, and the D2 pattern (Class III, 9*h*) with fivefold enrichment and 98% removal.

An additional piece of information on *s*-process elements in A + B grains was reported by Pellin et al. (2000*b*), who measured Mo isotopic ratios by RIMS in three A + B grains and also Zr ratios in two of them. The Mo ratios are normal, and none of the grains show the characteristic *s*-process isotopic pattern exhibited by mainstream grains (Nicolussi et al. 1998; Pellin et al. 1999). One grain has a substantial <sup>96</sup>Zr excess, the opposite of the depletion shown by mainstream grains (Nicolussi et al. 1997). These three grains lack any *s*-process signature. Unfortunately, these Zr and Mo isotopic analyses are currently restricted to three A + B grains with higher-than-solar <sup>14</sup>N/<sup>15</sup>N ratios and have not been performed on any grains with known trace element abundances.

#### 4. DISCUSSION

##### 4.1. Summary of the Properties of A + B Grains

Let us summarize the isotopic and elemental properties of the A + B grains before comparing them to astronomical observations of possible sources and discussing the nucleosynthetic processes that could possibly give rise to the isotopic and elemental compositions of the grains. A + B grains are defined as having <sup>12</sup>C/<sup>13</sup>C < 10 (Fig. 1). Their Si isotopic ratios are quite similar in their range and average to those of mainstream grains and differ only in details. The Si isotopic compositions of mainstream grains are believed to reflect primarily the initial compositions of their parent stars with little modification from subsequent nucleosynthetic processing. These initial compositions likely reflect the chemical evolution of the Galaxy (Alexander 1993; Timmes & Clayton 1996; Alexander & Nittler 1999; Lugaro et al. 1999), with stars of higher metallicity having on average higher <sup>29</sup>Si/<sup>28</sup>Si and <sup>30</sup>Si/<sup>28</sup>Si ratios. Comparison of the mainstream isotopic compositions with stellar models suggests that they formed in stars of approximately solar metallicity. The Y and Z grains, on the other hand, show <sup>30</sup>Si excesses relative to the mainstream correlation line and have lower average <sup>29</sup>Si/<sup>28</sup>Si and <sup>30</sup>Si/<sup>28</sup>Si ratios. These properties indicate an origin in lower-than-solar metallicity stars (Amari et al. 2001*b*; Hoppe et al. 1997*b*; Zinner et al. 2001). The similarity of Si isotopic ratios between the A + B grains and mainstream grains indicates that the A + B grains probably originated from stars with metallicity similar to that of mainstream grains, namely, close-to-solar metallicity.

The <sup>14</sup>N/<sup>15</sup>N ratios of A + B grains span a much wider range than those of mainstream grains, and a substantial

fraction have heavy N, i.e., <sup>14</sup>N/<sup>15</sup>N ratios smaller than solar (Fig. 1). Their inferred <sup>26</sup>Al/<sup>27</sup>Al ratios are, on average, higher than those of mainstream grains. With a few exceptions, titanium isotopic compositions of A + B grains show a similar range to those of mainstream grains, but with large error bars. As will be made clear in subsequent sections, there are major difficulties in identifying the stellar and nucleosynthetic sources of the A + B grains on the basis of their major and minor element (Si, C, N, and Al) isotopic compositions alone. Until a better understanding of these data is available, we think that it is premature to attempt to explain the isotopic data of the trace element Ti in the grains and will not discuss Ti any further.

Comparison of condensation calculations with the trace element patterns of the A + B grains indicates that seven A + B grains condensed from an atmosphere with solar abundances of *s*-process elements, while the other 12 grains show evidence of *s*-process enrichments of a factor of 3–5 compared with the solar system. It should be noted, however, that the KJH grains in which trace elements have been measured are not a representative sample of A + B grains. The range of their <sup>14</sup>N/<sup>15</sup>N ratios is much narrower (78–446) than that of all A + B grains (39–10,000), and grains with high <sup>14</sup>N/<sup>15</sup>N ratios (greater than 446) are not represented.

##### 4.2. Properties of Carbon Stars

The carbonaceous nature of SiC grains implies that they formed in a C-rich (C > O) atmosphere (Larimer & Bartholomay 1979; Lodders & Fegley 1997). Carbon-rich AGB stars of the N type have been identified as the most likely stellar sources of the mainstream SiC grains (Hoppe et al. 1994; Hoppe & Ott 1997) and proposed as the sources of Y and Z SiC grains (Amari et al. 2001*b*; Hoppe et al. 1997*b*; Zinner et al. 2001). The A + B grains must have originated from sources that allow condensation of SiC and that have <sup>12</sup>C/<sup>13</sup>C ratios compatible with those seen in the grains. In this section we consider all types of carbon stars as possible sources for the A + B grains and use isotopic and trace element abundances of the different carbon star types to narrow the types of A + B grain progenitor stars. We note that Clayton, Liu, & Dalgarno (1999) considered the condensation of carbonaceous dust from O-rich (O > C) ejecta from Type II SNe. However, the isotopic compositions of the A + B grains are so different from presolar grains that are identified to have an SN origin (Amari et al. 1992; Nittler et al. 1995, 1996; Travaglio et al. 1999*a*; Hoppe et al. 2000) that we exclude SNe as likely stellar sources for the A + B grains. Moreover, SNe can be ruled out on the basis of nucleosynthetic and stellar evolutionary models, as discussed below in § 4.3.

Table 3 summarizes the astronomically derived properties of several classes of carbon stars (for a detailed review of carbon stars see Wallerstein & Knapp 1998). Among them, R, J, and CH (giant and subgiant) stars and Sakurai's object have low <sup>12</sup>C/<sup>13</sup>C ratios. In this section we briefly sketch the properties of these stars. J stars are attractive sources for the A + B grains with normal *s*-process element abundances, while CH giant stars and Sakurai's object are candidates for the parent stars of grains enriched in *s*-process elements. A previous analysis of the stellar sources of all types of SiC grains, together with more detailed descriptions of carbon star properties, has been given by Lodders & Fegley (1998).

TABLE 3  
CARBON STAR PROPERTIES AND COMPARISON WITH A + B GRAINS

Parameters	C-N	C-J-N	C-R, C-J-R	C-H Low $^{12}\text{C}$	C-H High $^{12}\text{C}$	Subgiant CH	Ba II	Sakurai's Object <sup>a</sup>	HdC R CrB	A + B Grains
$T_{\text{eff}}$ (K)	$2650 \pm 250$ $\equiv 12$	$2650 \pm 250$ $\equiv 12$	$4560 \pm 200$ $\equiv 12$	$4950 \pm 300$ $\equiv 12$	$3630 \pm 80$ $\equiv 12$	$5740 \pm 420$ $\equiv 12$	$4600 \pm 300$ $\equiv 12$	$7500 \pm 300$ , cooling 9.7 <sup>b</sup>	$\sim 7000$ 7.21 <sup>b</sup>	...
$\epsilon\text{H}$	$-1.5$ to 3	0.5-5	$-0.5$ to 0.5	$-1$ to 0	?	$< 1.5$	$\sim 0.5$	3.6	?	...
$\epsilon\text{Li}$	8.75	8.72	9.08	...	...	8.82	8.67	9.7	9.61	...
$\epsilon\text{C}$	7.78	7.78	8.64	...	...	...	8.58	8.9	8.51	...
$\epsilon\text{N}$	8.7	8.62	8.86	...	...	8.78	8.76	9.5	9.01	...
$\epsilon\text{Fe}$	7.50	7.51	7.4	5-7	4.7	7.5-6.5	7-7.7	6.4	7.51	...
[Fe/H]	$-0.01$	0	$-0.1$	$-2.5$ to $-0.5$	$-2.85$	0 to $-1$	$-0.5$ to 0.2	$-0.7$ to $-0.2$	$= 0$	$\sim 0$
Tc	Some	No	No	No	No?	No	No	...	...	...
[s/Fe] <sup>c</sup>	1-2	0	0.2-0.3	0.5-1.3	2.1-2.6	0.5-1.2	0.3-1	2.2-3	...	Yes/No
[hs/Fe] <sup>d</sup>	1-2	0	0.2-0.3	1.5-2.5	2.7-3	0.2-0.8	0.3-1	...	...	Yes/No
[hs/s]	0	0	0	1-2	0.6-1	$-0.4$ to 0.1	$\sim 0$	$\leq 0.6$	...	...
C/O	1.14	1.15	1.7	1.2-8	1-2	$> 1.1$	0.7-0.96	...	4	$> 1$
C/N	9.3	8.7	2.75	0.5	...	...	1.23	...	13	...
$^{12}\text{C}/^{13}\text{C}$	30-80	3-10	4-15	$\sim 10$	$\geq 100$	$> 40$	8-33	1.5-5	$\sim 40-50$	2-10
$^{14}\text{N}/^{15}\text{N}$ <sup>e</sup>	$> 500$ , $\sim 5300$	$> 70$ , 150, $> 4000$	...	...	...	...	...	...	...	39-10,100
Population	Young disk	Young disk	Old disk	II, halo	II, halo	I, old disk	I, old disk	...	Old disk	...
$dM/dt$ ( $M_{\odot} \text{ yr}^{-1}$ )	$10^{-8}$ - $10^{-6}$	$10^{-8}$ - $10^{-7}$	...	...	...	...	...	...	...	...
CSE	SiC, carbon	SiC, carbon, sometimes silicate	Thin, if any	...	...	...	...	Graphite	Dust	...

<sup>a</sup> Data from 1996 May.

<sup>b</sup> Normalized to  $\log \Sigma \mu_i \epsilon_i = 12.15$ .

<sup>c</sup>  $s \equiv [\text{light } s\text{-process elements}/\text{Fe}] = \log (\text{light } s\text{-process elements}/\text{Fe})_{\text{star}} - \log (\text{light } s\text{-process elements}/\text{Fe})_{\odot}$ , where light  $s$ -process elements are Sr, Y, and Zr.

<sup>d</sup>  $hs \equiv [\text{heavy } s\text{-process elements}/\text{Fe}]$ , where heavy  $s$ -process elements are Ba and rare earth elements.

<sup>e</sup> Very uncertain.

4.2.1. *J Stars*

Since their initial description by Bouigue (1954), the J stars have remained a group of carbon stars that is poorly understood. The J stars are cool luminous stars located at the extreme red end of the Hertzsprung-Russell diagram, together with normal N-type carbon stars. Except for the strong  $^{13}\text{CN}$  and  $^{13}\text{C}_2$  bands (implying  $^{12}\text{C}/^{13}\text{C} < 10$ ) (Lambert et al. 1986; Ohnaka & Tsuji 1999) and solar *s*-process elemental abundances, they are indistinguishable from the normal N-type carbon stars. Bolometric magnitudes  $M_{\text{bol}}$  for J stars range from  $-8.7$  to  $-2.8$  and are comparable to those of N stars (Alksnis et al. 1998). Both J and N stars have similar effective temperatures, ranging from 2500 to 3000 K, and comparable CNO abundances and C/O ratios (e.g., Lambert et al. 1986). Spectral analysis of J stars by Utsumi (1985a, 1985b, 1988) and Abia & Isern (2000) reveals that the *s*-process elements are not enriched over other heavy elements (i.e.,  $[s/\text{Fe}] \sim \text{solar}$ ). The frequency of J stars among the cool carbon stars is estimated as 5%–15% (Lodders & Fegley 1998; Abia & Isern 2000).

The low  $^{12}\text{C}/^{13}\text{C}$  ratios and the solar abundance of the *s*-process elements indicate that CNO processing is operating in these stars and that the neutron-producing reaction  $^{13}\text{C}(\alpha, n)^{16}\text{O}$  is inoperable. However, CNO cycling should lead to high  $^{14}\text{N}$  abundances and to  $\text{C}/\text{O} < 1$ , which is not observed in J stars. Indeed, the CNO abundances are similar to those found for N stars, where dredge-up of  $^{12}\text{C}$  produced by shell He burning during thermal pulses is believed to be responsible for increasing the surface C/O ratio to higher than unity (however, *s*-elements, mostly produced by the  $^{13}\text{C}$  neutron source, are also dredged up and lead to the *s*-process enrichments found in N stars). Furthermore, the N abundances appear to be slightly subsolar in J and N stars. However, the N analyses may have problems (for a discussion see Lambert et al. 1986).

J stars, like N stars, are often surrounded by a circumstellar dust shell showing IR emission features characteristic of SiC. However, several J stars (5%–10%) also show silicate emission features (e.g., Little-Marenin 1986; Willems & de Jong 1986; Lloyd Evans 1990, 1991; Lambert, Hinkle, & Smith 1990; Barnbaum et al. 1991) and OH and  $\text{H}_2\text{O}$  maser emission from the shells around some stars (Nakada et al. 1987; Nakada, Deguchi, & Förster 1988). The origin of this oxygen-rich matter in the circumstellar shell is unclear.

The evolutionary status of J stars is also unclear, and several models have been proposed. Willems & de Jong (1986, 1988) have suggested that J stars are on the AGB and have recently converted from being O-rich to being C-rich as a result of the dredge-up of  $^{12}\text{C}$ . This could explain the presence of silicates from the time when the stars had  $\text{C}/\text{O} < 1$ . Such a history would be similar to the evolutionary sequence of normal cool giants (M–MS–S–N stars) where successive dredge-up of carbon increases the C/O ratio. However, this scenario does not work for J stars because it cannot explain the low  $^{12}\text{C}/^{13}\text{C}$  ratios (addition of  $^{12}\text{C}$  would increase this ratio), and one also expects enhancements in *s*-process elements, which are not observed. Furthermore, silicate dust is also expected to be found around some normal SC and N stars, but as far as we know, the presence of silicate dust around carbon stars is restricted to J stars.

Lloyd Evans (1990, 1991) has proposed that J stars underwent mass loss prior to or during the He core flash, while the envelope was still oxygen-rich. In order to explain

the silicate dust, he suggested that J stars with silicate emission may have an invisible companion and that some oxygen-rich dust is trapped in the accretion disk of such a low-mass companion. Abia & Isern (2000) have discussed the idea that binarity plays a role in the evolution of J stars. Tidal forces may cause strong nonstandard mixing between core and envelope during the He core flash. This can cause an enrichment of  $^{12}\text{C}$  in the envelope, and further CNO processing could reduce the  $^{12}\text{C}/^{13}\text{C}$  ratio. A similar process has been discussed by Dominy (1984) and McClure (1997) for the R stars (see below). However, the binary status of J stars is unclear.

4.2.2. *R Stars*

The R stars represent about half of all carbon stars. They are too hot for dust formation and do not exhibit IR excesses that would be generated by circumstellar dust. Therefore, we do not expect that any of the A+B grains originated from R stars. However, the R stars may provide clues to the origin of J stars. R stars share several properties with the J stars, which suggests that they might be the progenitors of J stars (e.g., Lloyd Evans 1986). Dominy (1984) has presented the most comprehensive study of 11 R stars and has shown that they have low  $^{12}\text{C}/^{13}\text{C}$  isotopic ratios (4–9, one with 15) and essentially no enrichments of *s*-process elements ( $s/\text{Fe} \sim 1$ –2 times solar). The major difference between J and R stars is that R stars are hotter (their effective temperatures are similar to those of G9–K2 giants) and that the range in C/O ratios (0.9–3) in R stars is larger than in the cooler J stars. That C/O ratios in R stars are higher than in J stars is not surprising in view of the fact that these stars lack dust shells and thus no depletion of carbon from the gas phase occurs by condensation, in contrast to J and N stars. Condensation leads to a gas-phase C/O ratio near unity. Since the C/O ratio is determined from analysis of the gas, the astronomically measured C/O ratios in J stars may not be representative for the entire envelope (for further discussion see Lodders & Fegley 1997).

The C and N abundances in R stars are above solar while  $[\text{O}/\text{Fe}]$  is normal, and Dominy (1984) has concluded that the CNO cycle operating near equilibrium cannot be responsible for  $\text{C}/\text{O} > 1$ . He suggested that abundances are established by a violent He core flash and subsequent mixing. In that case,  $^{12}\text{C}$  produced by He burning in the core is transported upward and experiences H burning. This could possibly increase the C/O ratio, decrease the  $^{12}\text{C}/^{13}\text{C}$  ratio, and also exclude neutron production by the  $^{13}\text{C}(\alpha, n)^{16}\text{O}$  reaction, so that *s*-processing does not occur. As mentioned above for the J stars, binarity may also play a role in the evolution of R stars. Radial velocity measurements by McClure (1997), however, have not revealed any evidence for binarity in 22 R stars, although on statistical grounds one would expect a frequency of about 20%, as known for normal G and K giants. McClure (1997) has suggested that R stars once were close binaries that coalesced during their evolution on the red giant or AGB.

4.2.3. *CH Stars*

Among carbon stars, there exist some peculiar stars with low  $^{12}\text{C}/^{13}\text{C}$  ratios whose *s*-process element abundances are clearly higher than solar (e.g., Vanture 1992a, 1992b, 1992c; Kipper & Kipper 1990; Kipper et al. 1996). The CH giants (fifth and sixth columns in Table 3) have effective tem-

peratures similar to those of R stars and are often classified as early R-type stars. However, abundance analyses reveal their special nature. Noticeable differences between CH stars and R stars are as follows. (1) CH stars are halo members, while R stars belong to the old disk population. (2) The metallicity of CH stars is low ( $[\text{Fe}/\text{H}]$  from  $-2.5$  to  $-0.5$ ), which is the reason why the CH band appears strong, since the opacity depends on metallicity. However, metallicities in R stars are only slightly subsolar ( $[\text{Fe}/\text{H}] \sim -0.1$ ). Some CH stars are among the stars with the lowest metallicity known (see, e.g., Barbuy et al. 1997). (3) Ratios of *s*-process element to Fe are 10–100 times solar in CH stars and approximately solar in R stars. (4) Almost all CH stars are binaries, while R stars are not.

CH giant stars fall into two subgroups, one with  $^{12}\text{C}/^{13}\text{C} < 10$ , consisting mainly of binaries, and another group represented by two stars with  $^{12}\text{C}/^{13}\text{C} > 90$ , which are probably not members of a binary system. The latter are also of lower metallicity with  $[\text{Fe}/\text{H}] \sim -2.8$ , while  $[\text{Fe}/\text{H}]$  values of stars from the first group range from  $-2.5$  to  $-0.5$ . References on CH stars are McClure (1985), Kipper & Kipper (1990), McClure & Woodsworth (1990), Tsuji et al. (1991), Kipper (1992), and Aoki & Tsuji (1997).

Here we focus on the CH stars with low  $^{12}\text{C}/^{13}\text{C}$  ratios. The discovery that essentially all such CH stars are binaries (McClure 1985; McClure & Woodsworth 1990) suggests that the abundance peculiarities in CH stars may be explained by mass transfer from an evolved companion. Mass transfer either proceeds via Roche lobe overflow or by accretion of stellar wind from the binary companion, which now is likely to be a white dwarf (e.g., Boffin & Jorissen 1988; Han et al. 1995).

This binary scenario is analogous to the scenario explaining the properties of Ba stars (eighth column in Table 3), which can be regarded as Population I analogs to the older Population II CH stars. The CH stars (and Ba stars) are unlikely to be on the AGB. Thus, their overabundances in carbon and *s*-process elements cannot be explained by thermal pulses during He burning. However, if these stars have more massive companions that already went through the AGB stage and “dumped” some of their envelope matter onto the star now seen as a CH (or Ba) star, the enrichments of C and *s*-process elements are easily understood. Once these contaminated stars reach their mass-loss stage, we may expect SiC formation as in normal carbon stars. In that case, the SiC grains should possess low  $^{12}\text{C}/^{13}\text{C}$  ratios and overabundances in *s*-process elements, as observed for about two-thirds of all A+B grains analyzed for trace elements.

CH stars are observed to have heavy *s*-process element enhancements that are larger than the enhancements of light *s*-process elements (i.e.,  $h_s > l_s$ ; for the definition of  $h_s$  and  $l_s$  see Table 3). It would be interesting to look for such a signature in presolar SiC grains by measuring  $h_s$  and  $l_s$  elements of roughly the same volatility (such as La and Y). The major problem with a CH origin of some A+B grains is that the CH stars are all metal-poor ( $[\text{Fe}/\text{H}] < -0.5$ ) (see Fig. 8), while the Si isotopes of these grains indicate that they come from sources of close-to-solar metallicity.

#### 4.2.4. Sakurai's Object

Sakurai's object (V4334 Sgr) was first discovered by the Japanese amateur astronomer Sakurai in 1996 and was originally thought to be a slow nova. Subsequent obser-

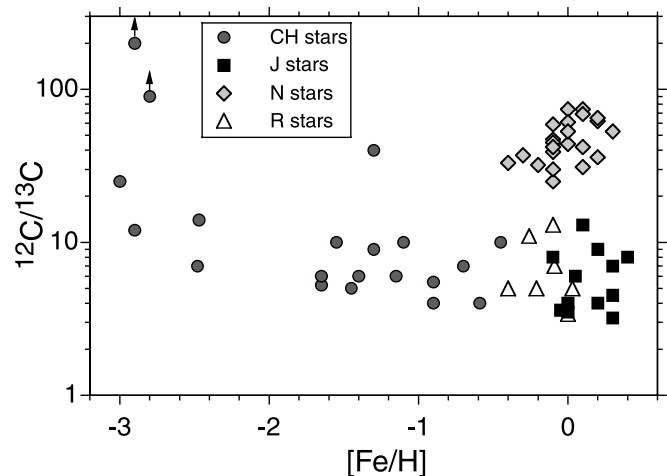


FIG. 8.—Carbon isotopic ratios observed in different classes of carbon stars are plotted against the metallicity  $[\text{Fe}/\text{H}]$ . J stars and R stars have close-to-solar metallicities as do N stars, which are believed to be the source of mainstream SiC grains. CH stars with  $^{12}\text{C}/^{13}\text{C} < 10$  have metallicities from  $-2$  to  $-0.5$ , whereas CH stars with high  $^{12}\text{C}/^{13}\text{C}$  ratios (greater than 90) are of low metallicity with approximately  $-2.8$ . Data are from Abia & Isern (2000), Aoki & Tsuji (1997), Dominy (1984), Hill et al. (2000), Kipper & Jorgensen (1994), Kipper & Kipper (1990), Kipper et al. (1996), Lambert et al. (1986), Ohnaka & Tsuji (1999), Tsuji et al. (1991), and Vanture (1992a, 1992b, 1992c).

vations, however, have revealed that it is a star undergoing a very late thermal pulse (VLTP) during the descent along the white dwarf cooling track. It is estimated that 10%–25% of the stars that go through a planetary nebula phase should experience a final He flash, producing a born-again giant (Renzini 1982; Iben 1984). The fact that this flash has been rarely observed must be due to the very short duration of the event. The lifetime of a born-again giant is estimated to be only 100–1000 yr (e.g., Asplund et al. 1999). The observed evolution of Sakurai's object indicates that the He flash event might in fact last only a few years (Herwig 2001).

The first spectroscopic observation by Duebeck & Benetti (1996) has shown that the object is C-, N-, and O-rich with  $\text{C} > \text{O}$ , but deficient in H. Later, high-resolution spectra taken by Asplund et al. (1997, 1999) together with the observations by Kipper & Klochkova (1997) have not only confirmed that Sakurai's object is H-deficient and C-rich but also revealed that it is enriched in the light *s*-process elements.

Asplund et al. (1999) have compiled the data taken between 1996 April and October (Asplund et al. 1997; Kipper & Klochkova 1997; Shetrone & Keane 1998) and summarized the observations. During this time span, H declined by a factor of 10 (mass fraction from  $7 \times 10^{-3}$  to  $7 \times 10^{-4}$ ), while Li and the light *s*-process elements increased by a factor of about 4. The abundances of He, C, N, O, and Ne stayed constant with  $\text{He}/\text{C}/\text{N}/\text{O}/\text{Ne} \approx 0.71/0.045/0.01/0.023/0.045$  (mass fractions). The object is slightly metal-poor ( $[\text{Fe}/\text{H}] = -0.7$  to  $-0.2$ ), and the observed  $^{12}\text{C}/^{13}\text{C}$  ratio is 1.5–5.0. The H deficiency and high He abundance are indicative of almost complete H burning. Furthermore, high Na and Al abundances ( $[\text{Na}/\text{Fe}] = 1.4$ ,  $[\text{Al}/\text{Fe}] = 1.0$ ) can be explained by proton capture on  $^{22}\text{Ne}$ ,  $^{25}\text{Mg}$ , and  $^{26}\text{Mg}$ . Further evidence of H burning is the large Li excess: the Li/H ratio ( $10^{-6.1}$  to  $10^{-4.8}$ ) exceeds the value observed in the most Li-rich AGB stars ( $10^{-8}$ ), suggesting that Li is produced by the Cameron-Fowler mecha-

nism (Cameron & Fowler 1971). The low  $^{12}\text{C}/^{13}\text{C}$  ratio coupled with those observations (especially the *s*-process enrichment) indicate that H burning has occurred in the envelope after the star left the AGB.

Sakurai's object has very high abundances of the light *s*-process elements such as Sr and Y ( $[\text{Sr}/\text{Fe}] = 3.0$ ,  $[\text{Y}/\text{Fe}] = 2.2$  in 1996 May). Such high abundances have not been observed in AGB or post-AGB stars, and it is possible that *s*-process nucleosynthesis occurred after the star left the AGB, although we cannot exclude the possibility that previously synthesized *s*-process material was mixed onto the surface during the born-again stage of the object.

Sakurai's object was observed to cool rapidly: the effective temperature was estimated to have been  $7500 \pm 300$  K in 1996 May, 6900 K in 1996 October (Asplund et al. 1997), and 5000–6000 K in 1998 (Asplund et al. 1999). This cooling is probably the result of stellar expansion caused by the energy released by the He flash and was accompanied by dust formation. *Infrared Space Observatory* (ISO) data taken in 1997 indicate the presence of graphite dust at a temperature of 680 K (Eyres et al. 1998). Since the ISO data taken for a full year between 1997 February and 1998 February show a strong and steadily increasing IR excess, Kerber et al. (1999) concluded that dust was continually produced in an extended, optically thin shell around the star. The spectra taken by the United Kingdom Infrared Telescope (UKIRT) in 1999 April and May suggest the presence of amorphous carbon with an estimated maximum size of  $0.6 \mu\text{m}$  (Tyne et al. 2000).

Theoretical work by Schönberner (1979) and Iben (1982) has shown that a star that descends the white dwarf cooling track can undergo a late He flash. A first attempt to investigate this evolutionary track and the “born-again” scenario qualitatively was undertaken by Iben et al. (1983). They showed that most of the H remaining in the star at the onset of the flash is incorporated into the He-burning convective shell and completely burned. Iben & MacDonald (1995) predicted the envelope of the star to be He-, C-, and N-rich with  $\text{He}/\text{C}/\text{N}/\text{O} = 300/20/6/1$  in relative numbers, or  $\text{He}/\text{C}/\text{N}/\text{O} = 0.76/0.15/0.05/0.01$  in mass fractions.

Herwig et al. (1999) and Herwig (2001) modeled Sakurai's object by investigating the evolutionary sequence of a low-mass ( $2 M_{\odot}$ ) star from the AGB through the post-AGB stage that experiences a very late thermal pulse. They found that in stars where shell H burning has already ceased (white dwarf cooling domain) the He flash-driven convection zone can extend into the H-rich envelope, leading to convective H burning. This process is estimated to last about a month before H in the envelope is completely consumed. The star's surface is still H-rich before the convective region reaches the envelope, but the convective H burning results in an H-free but He-, C-, and Ne-rich envelope with  $\text{He}/\text{C}/\text{O}/\text{Ne} = 0.38/0.35/0.22/0.035$  in mass fractions. While the  $^{12}\text{C}/^{13}\text{C}$  ratio is drastically reduced by H burning, the CNO cycle does not reach equilibrium before all of the available H is exhausted, and  $^{14}\text{N}$  remains much less abundant than  $^{12}\text{C}$ .

#### 4.2.5. *R Coronae Borealis Stars and HdC Stars*

*R Coronae Borealis* (R CrB) stars are He- and C-rich stars that are extremely deficient in H, and they belong to the group of hydrogen deficient (HdC) stars (e.g., Asplund et al. 2000). They possibly are closely related to Sakurai's object. Two scenarios have been proposed for their forma-

tion. The first involves the merger of a C-O white dwarf with an He white dwarf (Webbink 1984), and in the second scenario R CrB stars are born-again giants produced when a post-AGB star descending the white dwarf cooling track experiences a final thermal pulse (Renzini 1979; Asplund et al. 1997, 1998, 2000). In this second scenario R CrB stars represent an evolutionary stage after the born-again phase, one type of which (VLTP) is represented by Sakurai's object. Two other stars, Nova Aql 1919 (V605 Aql) and FG Sagittae (Blöcker & Schönberner 1997), are believed to have been observed while experiencing the late-type born-again phase. At present, it has not yet been decided which, if either, scenario applies or whether all R CrB stars are formed by the same process (see Asplund et al. 2000). Whatever the formation process, the fact that the nondetection of any  $^{12}\text{C}/^{13}\text{C}$  lines sets a lower limit of 40 for the  $^{12}\text{C}/^{13}\text{C}$  ratio in R CrB stars (Cottrell & Lambert 1982) eliminates them as parent stars for the A + B grains. Within the born-again scenario, the  $^{12}\text{C}/^{13}\text{C}$  ratio being substantially higher than in Sakurai's object can be explained by consumption of  $^{13}\text{C}$  during continued He burning after all the H has been exhausted. In fact, in the model by Herwig et al. (1999) and Herwig (2001), after cessation of H burning, the convective He shell grows again to engulf the region where H burning had taken place.

#### 4.2.6. *Conclusions from Stellar Observations*

On the basis of astronomical observations, J stars and born-again giants like Sakurai's object appear to be the most likely sources of A + B grains. Both have low  $^{12}\text{C}/^{13}\text{C}$  ratios and have been observed to produce C-rich dust. CH giants also have low  $^{12}\text{C}/^{13}\text{C}$  ratios but are excluded because of their low metallicity, and R stars are not known to produce any dust. Type J carbon stars do not have any *s*-process enrichments and thus could be the parent stars of A + B grains without any *s*-process signatures, while born-again giants could be the parent stars of grains with evidence for *s*-process enrichments. For the latter source it is difficult to estimate whether the number of these stars can account for the abundance of the grains. Sakurai's object produces dust copiously, but an important question is how much mass a born-again giant loses and how much dust it produces as long as the  $^{12}\text{C}/^{13}\text{C}$  ratio remains low.

#### 4.3. *Nucleosynthetic Considerations*

The isotopic compositions of the A + B grains must be the result of specific nucleosynthetic processes. In the following sections we discuss in which stellar environments these processes can take place.

The defining isotopic signature of the A + B grains is their low  $^{12}\text{C}/^{13}\text{C}$  ratio of less than 10. The only viable nuclear reaction that produces  $^{13}\text{C}$  is proton capture on preexisting  $^{12}\text{C}$  followed by  $\beta$ -decay:  $^{12}\text{C}(p, \gamma)^{13}\text{N}(\beta^+ \nu)^{13}\text{C}$ . In stars this happens during H burning in the CNO cycle at temperatures that can range from  $1.5 \times 10^7$  to  $3.5 \times 10^8$  K (hot CNO cycle). Whereas the equilibrium value for  $^{12}\text{C}/^{13}\text{C}$  is  $\sim 3.5$  and does not depend sensitively on temperature, the  $^{14}\text{N}/^{15}\text{N}$  ratio strongly depends on temperature and ranges from  $\sim 30,000$  at low temperatures to less than 0.1 at high temperatures. Hydrogen burning takes place in different types of stars at different stages during their evolution. Table 4 lists different stellar environments in which the CNO cycle can take place. However, what makes it so difficult to explain the low  $^{12}\text{C}/^{13}\text{C}$  ratios of the A + B grains is

TABLE 4  
SCENARIOS OF HYDROGEN BURNING<sup>a</sup>

Parameters	Core H Burning and First DU	CBP	HBB	Core He Flash	Sakurai's Object	Novae <sup>b</sup> CO	Novae <sup>b</sup> ONe	SNe <sup>c</sup> He/N Zone
<sup>12</sup> C/ <sup>13</sup> C .....	20	<10	<10	?	<10	0.3–4	0.3–4	8
C/O .....	<1	<1	<1, or ≥1	?	2.1	<1	<1	1.2
<sup>14</sup> N/ <sup>15</sup> N .....	900–1700	20000 (?)	32000	?	10000 <sup>d</sup>	2–30000	0.1–6	27000
<sup>26</sup> Al/ <sup>27</sup> Al .....	No <sup>26</sup> Al	?	0.001–0.045	?	?	0.1–1	0.1–1	0.24
<sup>29</sup> Si/ <sup>28</sup> Si .....	Initial	Initial	>Initial	Initial	>Initial	≤Initial	≤Initial	Initial
<sup>30</sup> Si/ <sup>28</sup> Si .....	Initial	Initial	>Initial	Initial	>Initial	Initial	≥Initial	Initial
s-process .....	No	No	Yes	No	Yes	No	No	No

<sup>a</sup> The isotopic and abundance properties of the first five scenarios are those of the envelope of stars where the processes take place. For example, the s-process does not occur in HBB; however, HBB occurs during third dredge-up episodes that enrich the envelope in s-process elements.

<sup>b</sup> The nova data are predicted values of nova ejecta from the one-dimensional hydrodynamical calculations by Kovetz & Priallnik 1997, Starrfield et al. 1997, J ose & Hernanz 1998, and J. J ose 2001, private communication.

<sup>c</sup> The SN data have been calculated for a 15  $M_{\odot}$  star with solar metallicity by Woosley & Weaver 1995.

<sup>d</sup> F. Herwig 2001, private communication.

that these ratios have to be present in the atmosphere of the stars from which the grains formed and that this atmosphere has to be C-rich ( $C > O$ ). The problem here is that in the CNO cycle most of the C is converted to <sup>14</sup>N and in equilibrium  $C < O$ .

In the following discussion we will encounter predictions for the <sup>14</sup>N/<sup>15</sup>N ratios of up to 20,000, significantly higher than the ratios measured in the grains, which are less than 10,000. We want to emphasize that contamination of SiC grains with isotopically normal N (<sup>14</sup>N/<sup>15</sup>N = 272) during the measurement will shift very high true <sup>14</sup>N/<sup>15</sup>N ratios toward lower ratios. Conversely, less-than-solar ratios could be shifted toward higher ratios, although this effect is expected to be much smaller.

Let us discuss the different scenarios that can produce low <sup>12</sup>C/<sup>13</sup>C ratios. We first consider low- to intermediate-mass stars with close-to-solar metallicity that started out with a solar <sup>12</sup>C/<sup>13</sup>C ratio of 89 and a <sup>14</sup>N/<sup>15</sup>N ratio of 272. The evolution of such stars has been described in detail (Iben 1977; El Eid 1994; Lattanzio & Boothroyd 1997; Lattanzio & Forestini 1999; Boothroyd & Sackmann 1999), and we can be brief. During the main-sequence phase, the CNO cycle occurs in the deep interior of the star (core H burning). However, this nucleosynthesis does not affect the composition of the star's surface until, after H exhaustion at the center of a star, the products of core H burning are mixed into the envelope during the first dredge-up and thus become observable. This results in a drop of the <sup>12</sup>C/<sup>13</sup>C ratio to ~20–25 and an increase of the <sup>14</sup>N/<sup>15</sup>N ratio to 900–1700, respectively (Iben 1977; El Eid 1994; Forestini & Charbonnel 1997; Boothroyd & Sackmann 1999). After the core ignites (violently in stars with less than 2.5  $M_{\odot}$ , an event called the core He flash), He burns in the convective core, while H continues to burn in a thin shell (shell burning). Intermediate-mass stars (greater than ~3.5  $M_{\odot}$ ) experience a second dredge-up when the convective envelope penetrates the extinguished H shell, bringing more H-burnt material to the surface. This changes the <sup>14</sup>N/<sup>15</sup>N ratio of the envelope to 1300–1900 but does not affect the <sup>12</sup>C/<sup>13</sup>C ratio significantly (El Eid 1994; Forestini & Charbonnel 1997).

However, it has been observed that red giants with masses of less than ~2.3  $M_{\odot}$  show lower <sup>12</sup>C/<sup>13</sup>C ratios than predicted to result from the first and second dredge-up (Lambert 1981; Sneden, Pilachowski, & Vandenberg 1986; Gilroy 1989; Gilroy & Brown 1991; Sneden 1991; Waller-

stein & Morell 1994). To explain these ratios, extra mixing has been invoked by Charbonnel (1994, 1995), subsequently called cool bottom processing (CBP) (Wasserburg et al. 1995), where material from the bottom of the envelope circulates into regions close to the H shell where some processing by H burning can take place. When this mechanism is taken into account, the <sup>12</sup>C/<sup>13</sup>C ratio of the envelope approaches the equilibrium value of the CN cycle, 3.5 (Charbonnel 1995).

With standard reaction rates, almost all the <sup>15</sup>N in the envelope is expected to be destroyed, resulting in a <sup>14</sup>N/<sup>15</sup>N ratio near the equilibrium ratio of ≥10,000 (Lattanzio & Boothroyd 1997). On the basis of simple calculations, Huss, Hutcheon, & Wasserburg (1997) found that subsolar <sup>14</sup>N/<sup>15</sup>N ratios could be reached by CBP if the <sup>18</sup>O( $p, \alpha$ )<sup>15</sup>N reaction rate at relevant energies was assumed to be much higher than that given by Caughlan & Fowler (1988). However, an increase by a factor of 1000 is required to account for the ratios in A+B grains, and such a large excursion from the generally accepted value is probably ruled out by experiments (e.g., Champagne & Pitt 1986).

Although the range of the <sup>12</sup>C/<sup>13</sup>C ratios expected from CBP agrees well with that observed in the A+B grains, it should be emphasized that all the processes discussed so far leave the surface of the star O-rich. Such a composition would not allow the condensation of SiC grains. Furthermore, stars during these evolutionary stages are not enriched in s-process elements. In the standard evolution models of low- to intermediate-mass stars the surface of the star becomes C-rich only during the AGB phase, when <sup>12</sup>C, synthesized by the triple- $\alpha$  reaction in the He-burning shell, is mixed into the envelope by recurring third dredge-up episodes. This increases the C/O ratio until it becomes greater than 1 and the star becomes a carbon star. However, this dredge-up inevitably also increases the <sup>12</sup>C/<sup>13</sup>C ratio, which is predicted to be much higher than 10 when  $C > O$ . The standard model of AGB star evolution thus does not produce low enough <sup>12</sup>C/<sup>13</sup>C ratios to explain the <sup>12</sup>C/<sup>13</sup>C ratios of the A+B grains, nor can it explain the low ratios observed in J-type carbon stars. On the other hand, the C and N isotopic ratios predicted for low-mass stars of solar metallicity generally agree with those of mainstream and type Y SiC grains (Hoppe et al. 1994; Gallino et al. 1994; Huss et al. 1997; Amari et al. 2001b).

Additional products of AGB nucleosynthesis are s-process elements, believed to be produced in the thin inter-

shell region between the H and He shells by neutron capture from the  $^{13}\text{C}(\alpha, n)^{16}\text{O}$  neutron source (Iben & Renzini 1982a, 1982b; Gallino et al. 1997, 1998). As discussed above, mainstream SiC grains carry a strong signature of this process (see, e.g., Hoppe & Ott 1997). In the model of Wasserburg et al. (1995) CBP might also occur in AGB stars during third dredge-up. If so, this could lead to the formation of a carbon star with  $\text{C} > \text{O}$  while  $^{12}\text{C}/^{13}\text{C}$  ratios are low. Ohnaka & Tsuji (1999) considered this as a possible scenario to produce J-type carbon stars. However, stars made in this way are expected to have *s*-process enhancements of the heavy elements, and J stars generally lack such enhancements. CBP is also expected to produce high  $^{14}\text{N}/^{15}\text{N}$  ratios [assuming the accepted value of the  $^{18}\text{O}(p, \alpha)^{15}\text{N}$  cross section], thus only A + B grains without *s*-process enhancements and with high  $^{14}\text{N}/^{15}\text{N}$  ratios could possibly come from AGB stars experiencing CBP. Furthermore, it remains to be seen whether more detailed models of such stars can produce carbon stars with low  $^{12}\text{C}/^{13}\text{C}$  ratios.

Another process that can lower the  $^{12}\text{C}/^{13}\text{C}$  ratio in the envelope of AGB stars is hot bottom burning (HBB). It occurs in model stars of intermediate mass (4–7  $M_{\odot}$ ) (Boothroyd, Sackmann, & Wasserburg 1995; Lattanzio & Forestini 1999). In such models, the base of the convective envelope reaches down into the H shell where the temperature is high enough for the CN cycle to operate.  $^{12}\text{C}$  is converted to  $^{13}\text{C}$  and  $^{14}\text{N}$ , decreasing the  $^{12}\text{C}/^{13}\text{C}$  ratio (down to  $\sim 3$ ) and increasing the  $^{14}\text{N}/^{15}\text{N}$  ratio (up to 30,000). This isotopic signature would match those of some of the A + B grains. However, HBB prevents the envelope from becoming C-rich as a result of the conversion of  $^{12}\text{C}$  into  $^{14}\text{N}$ , and SiC grains should not form. In rare cases, mostly in low-metallicity ( $Z = 0.004$ ) stars, He burning and third dredge-up might continue after HBB has stopped. In these cases,  $\text{C} > \text{O}$  can be obtained in the envelope while  $^{12}\text{C}/^{13}\text{C}$  ratios remain low (less than 10) (Frost et al. 1998; Lattanzio & Forestini 1999). Because mass loss is high during this short phase during the last thermal pulses (Frost et al. 1998), substantial amounts of carbonaceous grains could form, but the low metallicity required for such stars seems to exclude them as sources for A + B grains.

After leaving the AGB and becoming white dwarfs, 10%–25% of stars are believed to experience a late He flash and become born-again giants. Sakurai's object, described in detail in § 4.2.4, apparently is going through this stage. In this scenario, convective H burning via the CN cycle occurs when the He flash convective zone rich in freshly synthesized  $^{12}\text{C}$  extends into and is mixed with the H-rich envelope (Herwig et al. 1999; Herwig 2001). The reason that the envelope remains C-rich ( $\text{C} > \text{O}$ ) is that it is thin and the number of protons is limited so that the CN cycle never reaches equilibrium. The temperature at the bottom of the convective H burning zone, where most of the H burning takes place, is estimated to be  $1.15\text{--}1.5 \times 10^8$  K, the  $^{12}\text{C}/^{13}\text{C}$  ratio to be less than 10, and the  $^{14}\text{N}/^{15}\text{N}$  ratio to be higher than 10,000 (Herwig 2001; F. Herwig 2001, private communication). This temperature is somewhat higher than that achieved in the H-burning shell of AGB stars, which is estimated to be  $5\text{--}8 \times 10^7$  K (Forestini & Charbonnel 1997). Based on the isotopic signature, born-again giants like Sakurai's object are viable candidates for the parents of A + B grains with large  $^{14}\text{N}/^{15}\text{N}$  ratios. Presently, the VLTP models by Herwig do not consider any

neutron capture effects. Neutron capture might result in lower  $^{14}\text{N}$  and higher  $^{15}\text{N}$  abundances and thus lower  $^{14}\text{N}/^{15}\text{N}$  ratios (F. Herwig 2001, private communication). However, we have to await full stellar evolution models that consider the neutron capture reactions to see whether  $^{14}\text{N}/^{15}\text{N}$  ratios as low as those observed in the grains can be obtained.

A similar type of H burning, namely, mixing of material from the core He flash with the H-rich envelope and subsequent H burning, has been proposed to explain the C isotopic and elemental compositions of R stars (Dominy 1984) and J stars (Abia & Isern 2000). Hydrodynamic studies by Deupree and coworkers (Cole & Deupree 1980, 1981; Deupree 1984; Deupree & Wallace 1987) have shown that an off-center He flash can mix He-burning material into the H-rich envelope and the amount of  $^{12}\text{C}$  mixed to the surface could possibly make the star into a carbon star (Deupree & Wallace 1987). However, in order to explain the C isotopic composition of J stars, additional H burning has to convert a substantial fraction of the  $^{12}\text{C}$  into  $^{13}\text{C}$ , but at the same time the  $^{13}\text{C}(\alpha, n)$  neutron source cannot be activated to prevent the production of *s*-process elements. Full multidimensional models of the He flash including mixing with the envelope and with a nuclear network comprising the CNO elements (preferably up to Si) are necessary to determine whether all the right conditions can be achieved to match the properties of the J stars ( $\text{C} > \text{O}$ , low  $^{12}\text{C}/^{13}\text{C}$  ratios, no *s*-process enhancements). A similar scenario, mixing of protons into the He-burning region, in the first He flash during the double-shell burning phase of low-metallicity, low-mass RR Lyrae variables has recently been investigated (Cassisi, Castellanti, & Tornambè 1996). In such stars, all the H burns at a relatively high temperature. However, the extremely low metallicity ( $\log Z = -10$ ) of the stars undergoing this process eliminates them as possible parent stars for the A + B grains.

The temperatures of H burning in most of the scenarios considered so far (except for core H burning) are in the same range as those in the H-burning shell of AGB stars, namely,  $5\text{--}8 \times 10^7$  K (Forestini & Charbonnel 1997). The fundamental problem with all these scenarios (in addition to the problem that  $\text{C} < \text{O}$ ) is that at such temperatures, and even at the somewhat higher temperatures obtained for models of Sakurai's object, H burning via the CN(O) cycle produces very high  $^{14}\text{N}/^{15}\text{N}$  ratios (greater than 10,000) and the grains with low ratios cannot come from any of the stars where these processes take place. Hydrogen burning at much higher temperatures (hot H burning) takes place in novae. Nova explosions occur on the surface of a white dwarf onto which H-rich matter from a companion star in a binary system is accreted and compressed until a thermonuclear runaway occurs. Hydrodynamic calculations of novae have predicted low  $^{12}\text{C}/^{13}\text{C}$  ratios (around 0.3–4 for both CO and ONe novae), a wide range of  $^{14}\text{N}/^{15}\text{N}$  ratios (2–30,000 for CO novae, 0.1–6 for ONe novae), and high  $^{26}\text{Al}/^{27}\text{Al}$  ratios (0.1–1) (Kovetz & Prialnik 1997; José, Hernanz, & Coc 1997; José & Hernanz 1998; Starrfield, Gehrz, & Truran 1997; Starrfield et al. 1998). Novae are thus the only types of stars considered so far for which current models predict low  $^{14}\text{N}/^{15}\text{N}$  ratios. However, almost all nova models predict substantial anomalies in the Si isotopic ratios (deficits in  $^{29}\text{Si}$  and/or large excesses in  $^{30}\text{Si}$ ) and substantially lower  $^{14}\text{N}/^{15}\text{N}$  ratios than observed in the grains. A few presolar SiC grains and one graphite grain

have been identified as originating from novae (Amari et al. 2001a). They all have large  $^{30}\text{Si}$  excesses (Fig. 2). It is extremely unlikely that any of the A + B grains, whose Si isotopic ratios are to first order indistinguishable from those of mainstream SiC grains, have a nova origin.

Finally, let us consider massive stars that explode as Type II SNe. In such stars H burning via the CNO cycle has gone to completion in the He/N zone (for labeling of SN zones see Meyer, Weaver, & Woosley 1995). Figure 9 shows the  $^{12}\text{C}/^{13}\text{C}$  and  $^{14}\text{N}/^{15}\text{N}$  ratios predicted for this zone by the Woosley & Weaver (1995) model of a  $15 M_{\odot}$  star of solar metallicity. The average  $^{26}\text{Al}/^{27}\text{Al}$  ratio is 0.2, and this zone has  $\text{C} > \text{O}$ . The underlying layer is the He/C zone with very high  $^{12}\text{C}/^{13}\text{C}$  ratios and also  $\text{C} > \text{O}$ . At the bottom of this zone very low  $^{14}\text{N}/^{15}\text{N}$  ratios are predicted, as a result of neutrino reactions during the SN explosion. In order to investigate whether mixing between layers in these two zones can account for the C and N isotopic ratios of the A + B grains, we mix the layer with the lowest  $^{12}\text{C}/^{13}\text{C}$  ratio in the He/N zone with the layer with the highest  $^{12}\text{C}/^{13}\text{C}$  ratio in the He/C zone. The mixing line (solid black line in Fig. 9) misses most of the A + B grains, especially those with low  $^{14}\text{N}/^{15}\text{N}$  ratios. Some layers in the He/C zones have even lower  $^{14}\text{N}/^{15}\text{N}$  ratios than the layer with the highest  $^{12}\text{C}/^{13}\text{C}$  ratio, but these layers have low N concentrations, and the mixing line (gray line in Fig. 9) thus takes a com-

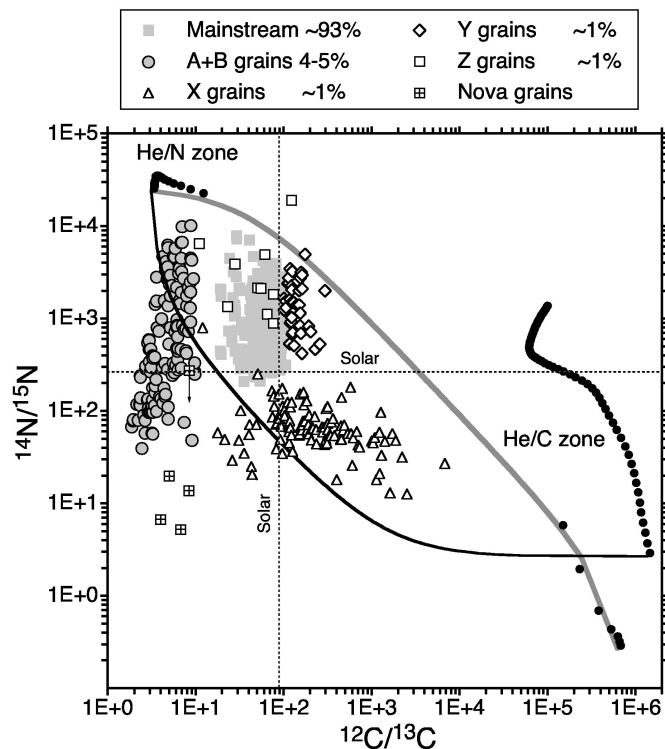


FIG. 9.—Nitrogen and carbon isotopic ratios of presolar SiC grains are compared to ratios predicted for the He/N zone and He/C zone of a  $15 M_{\odot}$  star of solar metallicity (Woosley & Weaver 1995). The two lines represent the isotopic ratios obtained when two layers from these two different zones are mixed. The paths of these lines depend not only on the isotopic ratios of the end components but also on their relative C and N abundances. For the mixing, the same layer in the He/N has been selected; the end component in the He/C zone generating the gray mixing line has a lower  $^{14}\text{N}/^{15}\text{N}$  ratio but a much higher C/N ratio than that giving rise to the black mixing line. Even the black mixing line misses most of the A + B grains.

pletely different path and runs essentially above all presolar SiC grains. It should be emphasized that the black mixing line represents a limiting case because most layers in the He/C zone have higher  $^{14}\text{N}/^{15}\text{N}$  ratios than the layer we chose. Zinner et al. (1998) and Travaglio et al. (1999a, 1999b) have shown that mixing of Type II SN ejecta fails to account for the low  $^{14}\text{N}/^{15}\text{N}$  ratios measured in SiC grains of type X, and, as can be seen in Figure 9, the situation is much worse for A + B grains with low  $^{14}\text{N}/^{15}\text{N}$  ratios.

In summary, H burning in the CN cycle can produce low  $^{12}\text{C}/^{13}\text{C}$  ratios and  $^{26}\text{Al}/^{27}\text{Al}$  ratios in the range observed in the grains, but to achieve this in stellar sources with  $\text{C} > \text{O}$  requires very special conditions so that the cycle cannot reach equilibrium. Most scenarios involve temperatures of less than  $10^8$  K, and at these temperatures  $^{14}\text{N}/^{15}\text{N}$  ratios are high and the low ratios observed in a sizeable fraction of the grains cannot be explained. Low  $^{14}\text{N}/^{15}\text{N}$  ratios are produced at much higher temperatures, believed to be present during nova explosions, but at these high temperatures H burning also affects the Si isotopes, and anomalies not seen in the A + B grains are predicted. Low  $^{14}\text{N}/^{15}\text{N}$  ratios are not only a problem for A + B grains but also for presolar grains from SNe (SiC grains of type X and low-density graphite grains) and have previously been discussed in detail (Zinner et al. 1998; Travaglio et al. 1999a, 1999b). SN grains and now the A + B grains indicate that the production of  $^{15}\text{N}$  is presently not well understood. It has been shown that massive stars produce more  $^{15}\text{N}$  if rotational mixing is taken into account (Heger 1998). That massive stars produce more  $^{15}\text{N}$  than is predicted by standard models is also supported by observations of  $^{15}\text{N}$  in the Large Magellanic Cloud and the galaxy NGC 4945 (Chin et al. 1999). In addition, as discussed above, Huss et al. (1997) showed that an increase of  $\sim 1000$  times in the  $^{18}\text{O}(p, \alpha)^{15}\text{N}$  reaction rate at relevant energies could lead to the observed  $^{14}\text{N}/^{15}\text{N}$  ratios during CBP. Although it is improbable that the true rate is that much higher than the currently accepted experimental value, a large extrapolation in energy from the experimental results to stellar energies is necessary, and it is certainly highly desirable to make measurements of the cross section at lower energies.

## 5. CONCLUSIONS

Presolar SiC grains of type A + B have low  $^{12}\text{C}/^{13}\text{C}$  ratios (less than 10), a large range of  $^{14}\text{N}/^{15}\text{N}$  ratios (39–10, 100), high inferred  $^{26}\text{Al}/^{27}\text{Al}$  ratios ( $\sim 10^{-3}$ ), and Si isotopic ratios slightly higher than solar. The Si isotopic distribution of the A + B grains is similar to that of mainstream grains, indicating that the A + B grains must have formed in stars of close-to-solar metallicity. Titanium isotopic compositions are broadly similar to those of mainstream SiC grains. Some grains seem to be enriched in s-process elements, others are not. No single known stellar source can account for all these isotopic and elemental signatures. Unlike other types of presolar SiC, such as mainstream, X, Y, Z, and nova grains, A + B grains most likely originated from more than one type of stellar objects. At present, it is difficult to assign A + B grains definitively to specific stellar sources because we do not have enough observational data of isotopic ratios (especially N) for most of the stellar objects discussed in § 4.2 and listed in Table 3. Furthermore, detailed theoretical models that can provide predictions of isotopic ratios are not yet available for many of these stars. For these reasons, we can only tentatively assign A + B

grains to stellar sources. For example, A + B grains with no *s*-process enrichment most likely formed in J stars, but we do not have any  $^{14}\text{N}/^{15}\text{N}$  ratio measurements in such stars. Grains with high  $^{14}\text{N}/^{15}\text{N}$  ratios and *s*-process enrichment could come from born-again giants such as Sakurai's object. CH stars with low  $^{12}\text{C}/^{13}\text{C}$  ratios, which have *s*-process enrichments, are less likely because they have low metallicities.

From a theoretical point of view, possible stellar sources of the A + B grains must have experienced both H and He burning. Helium burning is necessary to produce enough C, which has to be mixed into the envelope to produce a carbon star. However, the two processes have opposite effects on the  $^{12}\text{C}/^{13}\text{C}$  ratio and the C/O ratio in the envelope. Hydrogen burning decreases the  $^{12}\text{C}/^{13}\text{C}$  ratio but converts C into N, thus reducing the C/O ratio, while He burning adds  $^{12}\text{C}$  into the envelope and increases the  $^{12}\text{C}/^{13}\text{C}$  ratio. Thus, very special conditions, under which equilibrium of the CN cycle is not achieved, must be satisfied in order to obtain low  $^{12}\text{C}/^{13}\text{C}$  ratios and  $C > O$ .

A + B grains with high  $^{14}\text{N}/^{15}\text{N}$  ratios could be explained by CBP during the TP phase of low-mass AGB stars, but realistic stellar models have to be investigated to explore this possibility better. They could also be explained by HBB and continued third dredge-up after its termination (see Frost et al. 1998). However, these conditions seem to require low metallicity, in contrast to the grain data. Born-again giants such as Sakurai's object might be more likely sources. F. Herwig (2001, private communication) predicts high  $^{14}\text{N}/^{15}\text{N}$  ratios (greater than 10,000). These types of stars are expected to be enriched in *s*-process elements in the envelope. Unfortunately, we do not have any trace element data of A + B grains with  $^{14}\text{N}/^{15}\text{N}$  ratios higher than 500.

The low  $^{14}\text{N}/^{15}\text{N}$  ratios of some of the A + B grains and the large spread in N isotopic ratio remain unexplained by any of the possible scenarios except novae (Table 4) because they all predict high  $^{14}\text{N}/^{15}\text{N}$  ratios. Hot H burning produces both low  $^{12}\text{C}/^{13}\text{C}$  and  $^{14}\text{N}/^{15}\text{N}$  ratios. If this process takes place at a certain evolutionary stage of a star, the spread of  $^{14}\text{N}/^{15}\text{N}$  ratios can be explained by the mixing of hot H-burnt material and material that experienced CN burning at lower temperature. This hypothesis is consistent with the fact that the A + B grains with lower  $^{12}\text{C}/^{13}\text{C}$  grains tend to have lower  $^{14}\text{N}/^{15}\text{N}$  ratios and higher  $^{26}\text{Al}/^{27}\text{Al}$  ratios (see §§ 3.1 and 3.2). However, novae are the only known stellar source where hot H burning takes place, and

whether the process can occur during the evolution of "ordinary" stars is highly speculative. Furthermore, the temperature of the burning should be limited such that the C, N, and (to some extent) Al isotopes are affected, but not the Si isotopes.

The isotopic and elemental compositions of A + B grains provide new information about their possible parent stars that cannot be obtained in any other way. The fact that the grain data, especially low  $^{14}\text{N}/^{15}\text{N}$  ratios in conjunction with low  $^{12}\text{C}/^{13}\text{C}$  ratios and  $C > O$ , cannot be matched by existing theoretical models of nucleosynthesis and stellar evolution sets constraints on these models. For example, the data on A + B grains strengthen the conclusion previously reached in other studies (Zinner et al. 1998; Travaglio et al. 1999a, 1999b; Chin et al. 1999; Heger 1998) that the production of  $^{15}\text{N}$  is not well understood.

There are many things one would wish for in order to reach a better understanding of the problems presented by the A + B grains. It is highly desirable to measure the Mo isotopic ratios of grains with a range of C and N isotopic ratios in order to determine which of them carry *s*-process isotopic signatures. To date, only three B grains ( $^{12}\text{C}/^{13}\text{C} > 3.5$ ) with higher-than-solar  $^{14}\text{N}/^{15}\text{N}$  ratios have been analyzed. It is also highly desirable to obtain N isotopic ratios from J stars. If such stars are the parent stars of A + B grains with low  $^{14}\text{N}/^{15}\text{N}$  ratios, it might be possible to detect  $^{15}\text{N}$  in stars with ratios less than 100. Another item on the wish list are more theoretical efforts. The observation of Sakurai's object has triggered some theoretical activity to understand this phenomenon. We hope that the existence of the A + B grains and the measurement of their properties will have a similar effect. Finally, we also hope for more measurements of cross sections that are relevant to the C and N isotopic ratios produced by H burning. For example, new underground facilities should make it possible to extend measurements of the  $^{18}\text{O}(p, \alpha)^{15}\text{N}$  reaction rate to lower energies than has been possible so far.

We thank Mounib El Eid, Roberto Gallino, Falk Herwig, John Lattanzio, and Bradley Meyer for discussions about these enigmatic grains and Falk Herwig for providing unpublished data. Funding for visits by Mounib El Eid and John Lattanzio has been provided by the McDonnell Center for the Space Sciences. This work was supported by NASA grants NAG5-8336 (S. A. and E. Z.), NAG 5-4323 (K. L.), and NAG5-4297 (R. S. L.).

#### REFERENCES

- Abia, C., & Isern, J. 2000, *ApJ*, 536, 438  
 Alexander, C. M. O'D. 1993, *Geochim. Cosmochim. Acta*, 57, 2869  
 Alexander, C. M. O'D., & Nittler, L. R. 1999, *ApJ*, 519, 222  
 Alksnis, A., Balklavs, A., Dzervitis, U., & Eglitis, I. 1998, *A&A*, 338, 209  
 Amari, S., Anders, E., Virag, A., & Zinner, E. 1990, *Nature*, 345, 238  
 Amari, S., Gao, X., Nittler, L. R., Zinner, E., José, J., Hernanz, M., & Lewis, R. S. 2001a, *ApJ*, 551, 1065  
 Amari, S., Hoppe, P., Zinner, E., & Lewis, R. S. 1992, *ApJ*, 394, L43  
 ———, 1995a, *Meteoritics*, 30, 679  
 Amari, S., Lewis, R. S., & Anders, E. 1994, *Geochim. Cosmochim. Acta*, 58, 459  
 Amari, S., Nittler, L. R., Zinner, E., Gallino, R., Lugaro, M., & Lewis, R. S. 2001b, *ApJ*, 546, 248  
 Amari, S., Nittler, L. R., Zinner, E., & Lewis, R. S. 1996a, *Meteoritics Planet. Sci.*, 31, A6  
 ———, 1997, *Meteoritics Planet. Sci.*, 32, A6  
 ———, 1999, *Lunar Planet. Sci.*, 30, Abstract 1009 (Houston: Lunar Planet. Sci. Inst.), CD-ROM  
 ———, 2000, *Lunar Planet. Sci.*, 31, Abstract 1421 (Houston: Lunar Planet. Sci. Inst.), CD-ROM  
 Amari, S., Zinner, E., & Lewis, R. S. 1995b, *ApJ*, 447, L147  
 ———, 1996b, *ApJ*, 470, L101  
 Anders, E., & Grevesse, N. 1989, *Geochim. Cosmochim. Acta*, 53, 197  
 Anders, E., & Zinner, E. 1993, *Meteoritics*, 28, 490  
 Aoki, W., & Tsuji, T. 1997, *A&A*, 317, 845  
 Asplund, M., Gustafsson, B., Kameswara Rao, N., & Lambert, D. L. 1998, *A&A*, 332, 651  
 Asplund, M., Gustafsson, B., Lambert, D. L., & Kameswara Rao, N. 1997, *A&A*, 321, L17  
 ———, 2000, *A&A*, 353, 287  
 Asplund, M., Lambert, D. L., Kipper, T., Pollacco, D., & Shetrone, M. D. 1999, *A&A*, 343, 507  
 Barbuy, B., Cayrel, R., Spite, M., Beers, T. C., Spite, F., Nordström, B., & Nissen, P. E. 1997, *A&A*, 317, L63  
 Barnbaum, C., Kastner, J. H., Morris, M., & Likkel, L. 1991, *A&A*, 251, 79  
 Bernatowicz, T., Fraundorf, G., Tang, M., Anders, E., Wopenka, B., Zinner, E., & Fraundorf, P. 1987, *Nature*, 330, 728  
 Bernatowicz, T. J., Amari, S., Zinner, E., & Lewis, R. S. 1991, *ApJ*, 373, L73  
 Bernatowicz, T. J., Cowsik, R., Gibbons, P. C., Lodders, K., Fegley, B., Jr., Amari, S., & Lewis, R. S. 1996, *ApJ*, 472, 760

- Bernatowicz, T. J., & Zinner, E. 1997, in AIP Conf. Proc. 402, *Astrophysical Implications of the Laboratory Study of Presolar Materials*, ed. T. J. Bernatowicz & E. Zinner (New York: AIP), 750
- Blöcker, T., & Schönberner, D. 1997, *A&A*, 324, 991
- Boffin, H. M. J., & Jorissen, A. 1988, *A&A*, 205, 155
- Boothroyd, A. I., & Sackmann, I.-J. 1999, *ApJ*, 510, 232
- Boothroyd, A. I., Sackmann, I.-J., & Wasserburg, G. J. 1995, *ApJ*, 442, L21
- Bouigue, R. 1954, *Ann. d'Astrophys.*, 17, 104
- Cameron, A. G. W., & Fowler, W. A. 1971, *ApJ*, 164, 111
- Cassisi, S., Castellanti, V., & Tornambè, A. 1996, *ApJ*, 459, 298
- Caughlan, G. R., & Fowler, W. A. 1988, *At. Data Nucl. Data Tables*, 40, 283
- Champagne, A. E., & Pitt, M. L. 1986, *Nucl. Phys. A*, 457, 367
- Charbonnel, C. 1994, *A&A*, 282, 811
- . 1995, *ApJ*, 453, L41
- Chin, Y.-N., Henkel, C., Langer, N., & Mauersberger, R. 1999, *ApJ*, 512, L143
- Choi, B.-G., Huss, G. R., Wasserburg, G. J., & Gallino, R. 1998, *Science*, 282, 1284
- Choi, B.-G., Wasserburg, G. J., & Huss, G. R. 1999, *ApJ*, 522, L133
- Clayton, D. D., Liu, W., & Dalgarno, A. 1999, *Science*, 283, 1290
- Cole, P. W., & Deupree, R. G. 1980, *ApJ*, 239, 284
- . 1981, *ApJ*, 247, 607
- Cottrell, P. L., & Lambert, D. L. 1982, *ApJ*, 261, 595
- Deupree, R. G. 1984, *ApJ*, 287, 268
- Deupree, R. G., & Wallace, R. K. 1987, *ApJ*, 317, 724
- Dominy, J. F. 1984, *ApJS*, 55, 27
- Duerbeck, H. W., & Benetti, S. 1996, *ApJ*, 468, L111
- El Eid, M. 1994, *A&A*, 285, 915
- Eyres, S. P. S., Evans, A., Geballe, T. R., Salama, A., & Smalley, B. 1998, *MNRAS*, 298, L37
- Forestini, M., & Charbonnel, C. 1997, *A&AS*, 123, 241
- Frost, C. A., Cannon, R. C., Lattanzio, J. C., Wood, P. R., & Forestini, M. 1998, *A&A*, 332, L17
- Gallino, R., Arlandini, C., Busso, M., Lugaro, M., Travaglio, C., Straniero, O., Chieffi, A., & Limongi, M. 1998, *ApJ*, 497, 388
- Gallino, R., Busso, M., & Lugaro, M. 1997, in AIP Conf. Proc. 402, *Astrophysical Implications of the Laboratory Study of Presolar Materials*, ed. T. J. Bernatowicz & E. Zinner (New York: AIP), 115
- Gallino, R., Busso, M., Picchio, G., & Raiteri, C. M. 1990, *Nature*, 348, 298
- Gallino, R., Raiteri, C. M., & Busso, M. 1993, *ApJ*, 410, 400
- Gallino, R., Raiteri, C. M., Busso, M., & Matteucci, F. 1994, *ApJ*, 430, 858
- Gilroy, K. K. 1989, *ApJ*, 347, 835
- Gilroy, K. K., & Brown, J. A. 1991, *ApJ*, 371, 578
- Han, Z., Eggleton, P. P., Podsiadlowski, P., & Tout, C. A. 1995, *MNRAS*, 277, 1443
- Heger, A. 1998, Ph.D. thesis, Technische Universität München
- Herwig, F. 2001, *Ap&SS*, in press
- Herwig, F., Blöcker, T., Langer, N., & Driebe, T. 1999, *A&A*, 349, L5
- Hill, V., et al. 2000, *A&A*, 353, 557
- Hoppe, P., Amari, S., Zinner, E., Ireland, T., & Lewis, R. S. 1994, *ApJ*, 430, 870
- Hoppe, P., Annen, P., Strebler, R., Eberhardt, P., Amari, S., & Lewis, R. S. 1997a, *Lunar Planet. Sci.*, 28, 599
- Hoppe, P., Annen, P., Strebler, R., Eberhardt, P., Gallino, R., Lugaro, M., Amari, S., & Lewis, R. S. 1997b, *ApJ*, 487, L101
- Hoppe, P., & Ott, U. 1997, in AIP Conf. Proc. 402, *Astrophysical Implications of the Laboratory Study of Presolar Materials*, ed. T. J. Bernatowicz & E. Zinner (New York: AIP), 27
- Hoppe, P., Strebler, R., Eberhardt, P., Amari, S., & Lewis, R. S. 1996a, *Science*, 272, 1314
- . 1996b, *Lunar Planet. Sci.*, 27, 561
- . 2000, *Meteoritics Planet. Sci.*, 35, 1157
- Huss, G. R., Fahey, A. J., Gallino, R., & Wasserburg, G. J. 1994, *ApJ*, 430, L81
- Huss, G. R., Hutcheon, I. D., & Wasserburg, G. J. 1997, *Geochim. Cosmochim. Acta*, 61, 5117
- Hutcheon, I. D., Huss, G. R., Fahey, A. J., & Wasserburg, G. J. 1994, *ApJ*, 425, L97
- Iben, I., Jr. 1977, in *Advanced Stages in Stellar Evolution*, ed. P. Bouvier & A. Maeder (Sauverny: Genève Obs.), 1
- . 1982, *ApJ*, 260, 821
- . 1984, *ApJ*, 277, 333
- Iben, I., Jr., Kaler, J. B., Truran, J. W., & Renzini, A. 1983, *ApJ*, 264, 605
- Iben, I., Jr., & MacDonald, J. 1995, in *White Dwarfs*, ed. D. Koester & K. Werner (Berlin: Springer), 443, 48
- Iben, I., Jr., & Renzini, A. 1982a, *ApJ*, 259, L79
- . 1982b, *ApJ*, 263, L23
- José, J., & Hernanz, M. 1998, *ApJ*, 494, 680
- José, J., Hernanz, M., & Coc, A. 1997, *ApJ*, 479, L55
- Kerber, F., Blommaert, J. A. D. L., Groenewegen, M. A. T., Kimeswenger, S., Käufel, H. U., & Asplund, M. 1999, *A&A*, 350, L27
- Kipper, T. 1992, *Baltic Astron.*, 1, 181
- Kipper, T., & Jorgensen, U. G. 1994, *A&A*, 290, 148
- Kipper, T., Jorgensen, U. G., Klochkova, V. G., & Panchuk, V. E. 1996, *A&A*, 306, 489
- Kipper, T., & Klochkova, V. G. 1997, *A&A*, 324, L65
- Kipper, T. A., & Kipper, M. A. 1990, *Soviet Astron. Lett.*, 16, 478
- Kovetz, A., & Prialnik, D. 1997, *ApJ*, 477, 356
- Lambert, D. L. 1981, in *Physical Processes in Red Giants*, ed. I. Iben, Jr. & A. Renzini (Dordrecht: Reidel), 115
- Lambert, D. L., Gustafsson, B., Eriksson, K., & Hinkle, K. H. 1986, *ApJS*, 62, 373
- Lambert, D. L., Hinkle, K. H., & Smith, V. V. 1990, *AJ*, 99, 1612
- Larimer, J. W., & Bartholomay, M. 1979, *Geochim. Cosmochim. Acta*, 43, 1455
- Lattanzio, J., & Forestini, M. 1999, in *Asymptotic Giant Branch Stars*, ed. T. Le Bertre, A. Lèbre, & C. Waelkens (Provo: ASP), 31
- Lattanzio, J. C., & Boothroyd, A. I. 1997, in AIP Conf. Proc. 402, *Astrophysical Implications of the Laboratory Study of Presolar Materials*, ed. T. J. Bernatowicz & E. Zinner (New York: AIP), 85
- Lewis, R. S., Amari, S., & Anders, E. 1990, *Nature*, 348, 293
- . 1994, *Geochim. Cosmochim. Acta*, 58, 471
- Lewis, R. S., Tang, M., Wacker, J. F., Anders, E., & Steel, E. 1987, *Nature*, 326, 160
- Little-Marenin, I. R. 1986, *ApJ*, 307, L15
- Lloyd Evans, T. 1986, *MNRAS*, 220, 723
- . 1990, *MNRAS*, 243, 336
- . 1991, *MNRAS*, 249, 409
- Lodders, K., & Fegley, B., Jr. 1995, *Meteoritics*, 30, 661
- . 1997, in AIP Conf. Proc. 402, *Astrophysical Implications of the Laboratory Study of Presolar Materials*, ed. T. J. Bernatowicz & E. Zinner (New York: AIP), 391
- . 1998, *Meteoritics Planet. Sci.*, 33, 871
- Lugaro, M., Zinner, E., Gallino, R., & Amari, S. 1999, *ApJ*, 527, 369
- McClure, R. D. 1985, *JRASC*, 79, 277
- . 1997, *PASP*, 109, 256
- McClure, R. D., & Woodsworth, A. W. 1990, *ApJ*, 352, 709
- Meyer, B. S., Weaver, T. A., & Woosley, S. E. 1995, *Meteoritics*, 30, 325
- Nakada, Y., Deguchi, S., & Forster, J. R. 1988, *A&A*, 193, L13
- Nakada, Y., Izumiura, H., Onaka, T., Hashimoto, O., Ukita, N., Deguchi, S., & Tanabe, T. 1987, *ApJ*, 323, L77
- Nicolussi, G. K., Davis, A. M., Pellin, M. J., Lewis, R. S., Clayton, R. N., & Amari, S. 1997, *Science*, 277, 1281
- Nicolussi, G. K., Pellin, M. J., Lewis, R. S., Davis, A. M., Amari, S., & Clayton, R. N. 1998, *Geochim. Cosmochim. Acta*, 62, 1093
- Nittler, L. R. 1996, Ph.D. thesis, Washington Univ.
- Nittler, L. R., Alexander, C. M. O'D., Gao, X., Walker, R. M., & Zinner, E. K. 1994, *Nature*, 370, 443
- . 1997, *ApJ*, 483, 475
- Nittler, L. R., Amari, S., Zinner, E., Woosley, S. E., & Lewis, R. S. 1996, *ApJ*, 462, L31
- Nittler, L. R., et al. 1995, *ApJ*, 453, L25
- Ohnaka, K., & Tsuji, T. 1999, *A&A*, 345, 233
- Ott, U., & Begemann, F. 1990, *ApJ*, 353, L57
- Pellin, M. J., Calaway, W. F., Davis, A. M., Lewis, R. S., Amari, S., & Clayton, R. N. 2000a, *Lunar Planet. Sci.*, 31, Abstract 1917 (Houston: Lunar Planet. Sci. Inst.), CD-ROM
- Pellin, M. J., Davis, A. M., Calaway, W. F., Lewis, R. S., Clayton, R. N., & Amari, S. 2000b, *Lunar Planet. Sci.*, 31, Abstract 1934 (Houston: Lunar Planet. Sci. Inst.), CD-ROM
- Pellin, M. J., Davis, A. M., Lewis, R. S., Amari, S., & Clayton, R. N. 1999, *Lunar Planet. Sci.*, 30, Abstract 1969 (Houston: Lunar Planet. Sci. Inst.), CD-ROM
- Podosek, F. A., Prombo, C. A., Amari, S., & Lewis, R. S. 2001, *ApJ*, in press
- Prombo, C. A., Podosek, F. A., Amari, S., & Lewis, R. S. 1993, *ApJ*, 410, 393
- Renzini, A. 1979, in *Stars and Star Systems*, ed. B. E. Westerlund (Dordrecht: Reidel), 155
- . 1982, in *Wolf-Rayet Stars: Observations, Physics, Evolution*, ed. C. W. H. de Loore & A. J. Willis (Dordrecht: Reidel), 413
- Richter, S., Ott, U., & Begemann, F. 1993, in *Nuclei in the Cosmos*, ed. F. Käppeler & K. Wisshak (Bristol and Philadelphia: Institute of Physics Publ.), 127
- Schönberner, D. 1979, *A&A*, 79, 108
- Shetrone, M. D., & Keane, M. 1998, in *3d Conf. on Faint Blue Stars*, ed. A. G. Davis-Philip, J. W. Liebert, R. A. Saffer, & D. S. Hayes (Scheneectady: Davis), 505
- Snedden, C. 1991, in *Evolution of Stars: The Photospheric Abundance Connection*, ed. G. Michaud & A. Tutukov (Netherlands: IAU), 235
- Snedden, C., Pilachowski, C. A., & Vandenberg, D. A. 1986, *ApJ*, 311, 826
- Starrfield, S., Gehr, R. D., & Truran, J. W. 1997, in AIP Conf. Proc. 402, *Astrophysical Implications of the Laboratory Study of Presolar Materials*, ed. T. J. Bernatowicz & E. Zinner (New York: AIP), 203
- Starrfield, S., Truran, J. W., Wiescher, M. C., & Sparks, W. M. 1998, *MNRAS*, 296, 502
- Tang, M., & Anders, E. 1988, *Geochim. Cosmochim. Acta*, 52, 1235
- Timmes, F. X., & Clayton, D. D. 1996, *ApJ*, 472, 723
- Travaglio, C., Gallino, R., Amari, S., Zinner, E., Woosley, S., & Lewis, R. S. 1999a, *ApJ*, 510, 325
- Travaglio, C., Gallino, R., Zinner, E., Amari, S., & Woosley, S. 1999b, in *Nuclei in the Cosmos V*, ed. N. Prantzos (Paris: Editions Frontières), 567
- Tsuji, T., Iye, M., Tomioka, K., Okada, T., & Sato, H. 1991, *A&A*, 252, L1
- Tyne, V. H., Eyres, S. P. S., Geballe, T. R., Evans, A., Smalley, B., Duerbeck, H. W., & Asplund, M. 2000, *MNRAS*, 315, 595
- Utsumi, K. 1985a, *Proc. Japan Acad.*, 61B, 193

- Utsumi, K. 1985b, in *Cool Stars with Excesses of Heavy Elements*, ed. M. Jaschek & P. C. Keenan (Dordrecht: Reidel), 243
- . 1988, in *Atmospheric Diagnostics of Stellar Evolution: Chemical Peculiarity, Mass Loss, and Explosion*, ed. K. Nomoto (Berlin and New York: Springer), 44
- Vanture, A. D. 1992a, *AJ*, 103, 2035
- . 1992b, *AJ*, 104, 1986
- . 1992c, *AJ*, 104, 1997
- Wallerstein, G., & Knapp, G. R. 1998, *ARA&A*, 36, 369
- Wallerstein, G., & Morell, O. 1994, *A&A*, 281, L37
- Wasserburg, G. J., Boothroyd, A. I., & Sackmann, I.-J. 1995, *ApJ*, 447, L37
- Webbink, R. F. 1984, *ApJ*, 277, 355
- Willems, F. J., & de Jong, T. 1986, *ApJ*, 309, L39
- . 1988, *A&A*, 196, 173
- Woosley, S. E., & Weaver, T. A. 1995, *ApJS*, 101, 181
- Zinner, E. 1998, *Annu. Rev. Earth Planet. Sci.*, 26, 147
- Zinner, E., Amari, S., Gallino, R., & Lugaro, M. 2001, *Nucl. Phys. A*, 688, 102
- Zinner, E., Amari, S., & Lewis, R. S. 1991, *ApJ*, 382, L47
- Zinner, E., Amari, S., Nittler, L. R., Travaglio, C., Gallino, R., Woosley, S., & Lewis, R. S. 1998, *Lunar Planet. Sci.*, 29, Abstract 1763 (Houston: Lunar Planet. Sci. Inst.), CD-ROM
- Zinner, E., Tang, M., & Anders, E. 1989, *Geochim. Cosmochim. Acta*, 53, 3273